

## 7-Aminopyrazolo[1,5-*a*]pyrimidines as Potent Multitargeted Receptor Tyrosine Kinase Inhibitors

Robin R. Frey,\* Michael L. Curtin, Daniel H. Albert, Keith B. Glaser, Lori J. Pease, Niru B. Soni, Jennifer J. Bouska, David Reuter, Kent D. Stewart, Patrick Marcotte, Gail Bukofzer, Junling Li, Steven K. Davidsen, and Michael R. Michaelides

Global Pharmaceutical Research and Development, Abbott Laboratories, 100 Abbott Park Road, Abbott Park, Illinois 60064-6100

Received November 7, 2007

7-Aminopyrazolo[1,5-*a*]pyrimidine urea receptor tyrosine kinase inhibitors have been discovered. Investigation of structure–activity relationships of the pyrazolo[1,5-*a*]pyrimidine nucleus led to a series of 6-(4-*N,N'*-diphenyl)ureas that potently inhibited a panel of vascular endothelial growth factor receptor (VEGFR) and platelet-derived growth factor receptor (PDGFR) kinases. Several of these compounds, such as **34a**, are potent inhibitors of kinase insert domain-containing receptor tyrosine kinase (KDR) both enzymatically (<10 nM) and cellularly (<10 nM). In addition, compound **34a** possesses a favorable pharmacokinetic profile and demonstrates efficacy in the estradiol-induced murine uterine edema (UE) model (ED<sub>50</sub> = 1.4 mg/kg).

### Introduction

Protein kinase signaling is a predominant means of signal transduction in eukaryotic cells and controls processes such as proliferation, migration, survival, and cell cycle progression. Misregulation of these tightly controlled processes through mutation or overexpression of kinases is implicated in a number of disease states including cancer and immunological disorders.<sup>1,2</sup>

Angiogenesis, the process by which new capillaries are formed from existing blood vessels, is essential for a tumor to grow beyond about 1–2 mm.<sup>3</sup> As a tumor becomes larger, it becomes increasingly hypoxic, leading to induction of growth factors, including vascular endothelial growth factor (VEGF<sup>α</sup>),<sup>1</sup> which trigger angiogenesis.<sup>4,5</sup> Once angiogenesis has been induced, the tumor becomes highly vascularized and can grow at a much more rapid pace.<sup>6</sup> Although VEGF-stimulated angiogenesis is crucial for embryonic neovascularization,<sup>7</sup> in adults its normal physiologic roles are largely restricted to reproductive function and wound healing,<sup>8</sup> suggesting that inhibition of angiogenesis may present an opportunity for the selective treatment of cancer.<sup>9</sup> Approval by the U.S. Food and Drug Administration of the anti-VEGF antibody bevacizumab,<sup>10</sup> along with the clinical efficacy shown by this agent, has further heightened interest in identifying small-molecule inhibitors of angiogenic kinases.

VEGF, as well as other proangiogenic growth factors including platelet-derived growth factor (PDGF), acts through binding to receptor tyrosine kinases (RTKs), a family of transmembrane proteins. Upon binding the growth factor, RTKs dimerize and undergo autophosphorylation, triggering a series of downstream events leading to proliferation, migration, and cell survival.<sup>11</sup>

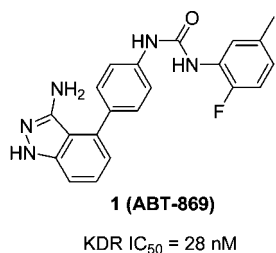
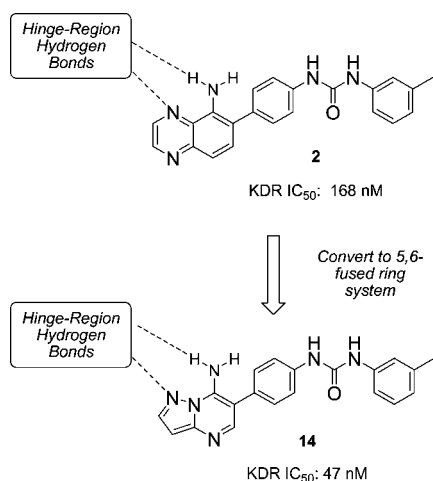
VEGF promotes angiogenesis through binding to a family of homologous VEGF receptors, including KDR (VEGFR-2), Flt-1 (VEGFR-1), and Flt-4 (VEGFR-3). Likewise, PDGF binds to the PDGFR family of receptors, Flt-3, PDGFRβ, cKit, and CSF1R (colony-stimulating factor 1 receptor). The PDGF receptors not only trigger angiogenesis but also contribute to tumor growth.<sup>12</sup>

Early work in the field of receptor tyrosine kinase inhibitors was directed toward the identification of agents with a high degree of selectivity for a particular enzyme.<sup>13,14</sup> This led to the discovery of first-generation RTK inhibitors, including compounds such as SU5416 ((*Z*)-3-((3,5-dimethyl-1*H*-pyrrol-2-yl)methylene)indolin-2-one),<sup>15,16</sup> a small molecule that is selective for VEGFR. Later research, however, suggests that compounds targeting a broader range of RTKs may lead to a more robust antitumor response, as there are a number of redundant RTK-mediated processes that can promote angiogenesis.<sup>17,18</sup> Furthermore, recent data show that tumors treated with selective agents can develop resistance through the up-regulation of alternative kinase-mediated pathways.<sup>19</sup> This has led to the development of broader-spectrum RTK inhibitors, including two recently launched anticancer drugs, SU11248 ((*Z*)-*N*-(2-(diethylamino)ethyl)-2,4-dimethyl-5-((5-methyl-2-oxoindolin-3-ylidene)methyl)-1*H*-pyrrole-3-carboxamide),<sup>20</sup> an inhibitor of KDR, Flt-1, PDGFR, and c-Kit, and BAY 43-9006 (*N*-[4-chloro-3-(trifluoromethyl)phenyl]-*N'*-[4-[2-(*N*-methylcarbamoyl)-4-pyridyloxy]phenyl]urea),<sup>21</sup> an inhibitor of Raf kinase, as well as of the VEGFR, EGFR, and PDGFR kinases.

Our laboratories have been engaged in research directed toward multitargeted RTK inhibitors, including thienopyrimidines,<sup>22</sup> isoindolinone ureas,<sup>23</sup> and aminoindazole ureas including **1** (Figure 1).<sup>24</sup> In light of the efficacy observed for RTK inhibitors in the clinic,<sup>25</sup> we are continuing our efforts to identify structurally novel kinase inhibitor classes. Rational design efforts in our laboratories identified aminoquinoxaline **2**, which was a submicromolar inhibitor of KDR (IC<sub>50</sub> = 168 nM). Brief SAR study based on the quinoxaline scaffold failed to generate compounds with substantially improved potency, so we sought other templates that might exploit a binding mode similar to that proposed for compound **2**, in which the biarylurea extends into the hydrophobic pocket and the bicyclic core forms

\* To whom correspondence should be addressed. Phone: (847) 938-2517. Fax: (847) 935-5165. E-mail: robin.r.frey@abbott.com.

<sup>a</sup> Abbreviations: ATP, adenosine 5' triphosphate; CSF1R, colony-stimulating factor-1; DMF-DMA, dimethylformamide dimethyl acetal; EDCI, *N*-(3-dimethylaminopropyl)-*N'*-ethylcarbodiimide hydrochloride; EGFR, endothelial growth factor receptor; Flt-1, fms-like tyrosine kinase-1; Flt-3, fms-like tyrosine kinase 3; KDR, kinase insert domain-containing receptor tyrosine kinase; PDGF, platelet-derived growth factor; PDGFR, platelet-derived growth factor receptor; RTK, receptor tyrosine kinase; SAR, structure–activity relationship; UE, estradiol-induced murine uterine edema assay; VEGF, vascular endothelial growth factor; VEGFR, vascular endothelial growth factor receptor.

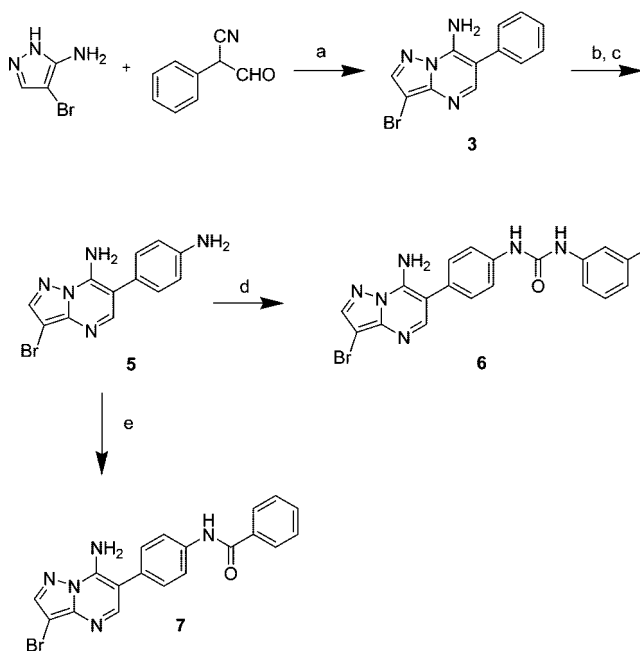
**Figure 1.** Compound 1.**Figure 2.** Lead structure **2** and pyrazolo[1,5-*a*]pyrimidine **14**.

hydrogen bonds to the hinge region of the enzyme as shown in Figure 2.<sup>26</sup> Modification of the aminoquinoxaline lead structure led to the identification of a series of 7-aminopyrazolo[1,5-*a*]pyrimidine inhibitors of KDR such as **14**, which demonstrated improved potency. In this paper, we describe the synthesis and characterization of this novel series of 7-aminopyrazolo[1,5-*a*]pyrimidines as potent inhibitors of the VEGFR and PDGFR tyrosine kinases.<sup>27</sup>

## Chemistry

Our initial synthetic route, shown in Scheme 1, began with the cyclocondensation of 3-amino-4-bromopyrazole with 3-oxo-2-phenylpropanenitrile under acidic conditions to give the fused bicyclic aromatic heterocycle **3**.<sup>28</sup> This compound was then subjected to electrophilic aromatic nitration yielding a mixture of nitration products favoring the para isomer, followed by reduction of the nitro group to give aniline **5**, which was treated with *m*-tolyl isocyanate to give the urea **6**. Similar conditions were used to prepare urea derivatives **6a–c** (Table 3); amide **7** (Table 1) was prepared by an amide coupling of **5** with benzoic acid. The 7-*des*-amino analogue **10** was prepared in an analogous fashion from 2-phenylmalonaldehyde, as shown in Scheme 2. Compounds **4** and **41** (Tables 1 and 4, respectively), which bear a 4-methoxy group in place of the urea, were prepared using cyclocondensation conditions similar to those described in Schemes 1 and 2, respectively, starting with commercially available 3-(4-methoxyphenyl)-3-oxopropanenitrile.

It was envisioned that the bromine atom in compound **3** would serve not only as a blocking group to prevent potential nitration at the 3-position of the pyrazole but also as a handle allowing for subsequent functionalization of the molecule using palladium-catalyzed coupling chemistry. In practice, however, neither the bromide **3** nor the analogous iodide would undergo

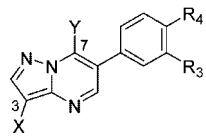
**Scheme 1.** Synthesis of 7-Aminopyrazolo[1,5-*a*]pyrimidines **6** and **7** via Nitration<sup>a</sup>

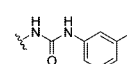
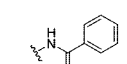
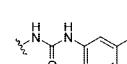
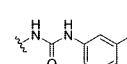
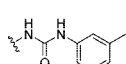
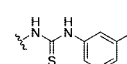
<sup>a</sup> Conditions: (a) concentrated HCl, EtOH, reflux, 74%; (b) HNO<sub>3</sub>, H<sub>2</sub>SO<sub>4</sub>, -20 °C to room temp; (c) Fe<sup>0</sup>, NH<sub>4</sub>Cl, THF, EtOH, H<sub>2</sub>O, 80 °C, 29% (two-step yield); (d) *m*-tolyl isocyanate, DMF, -20 °C to room temp, 47%; (e) benzoic acid, EDCI, HOBt, *N*-methylmorpholine, DMF, 60%.

Suzuki or Sonogoshira couplings. A variety of catalysts as well as high-temperature microwave reaction conditions were employed,<sup>29</sup> but these compounds would not undergo palladium-catalyzed coupling reactions even following Boc protection of the amino functionality. Similar couplings have been reported for 3-bromo pyrazolo[1,5-*a*]pyrimidines lacking the 7-amino substituent,<sup>30</sup> and we observed that compound **41** (Table 4) underwent facile Suzuki coupling with thiophene-3-boronic acid.

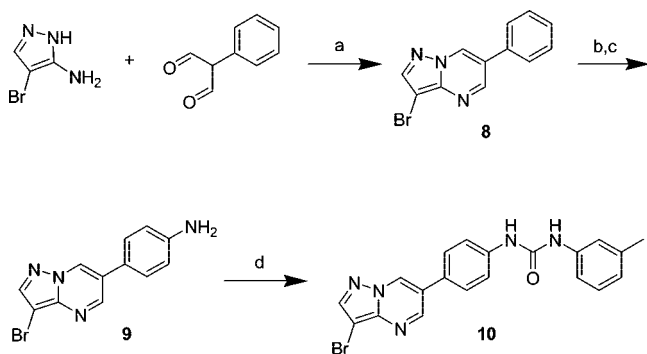
Upon discovering that bromide **3** could not be elaborated through palladium-catalyzed cross-coupling reactions, it became necessary to find an alternative route that would allow for the substitution of a broad range of substituents on the pyrazole and that would also incorporate a nitro group on the 6-phenyl ring prior to the cyclocondensation, thereby alleviating the need to perform a nitration on a more highly functionalized system. The optimized synthesis of 7-aminopyrazolo[1,5-*a*]pyrimidines incorporating a diphenylurea substituent in the 6-position is typified by the preparation of compound **14**, shown in Scheme 3. 4-Nitrophenylacetonitrile was treated with dimethylformamide-dimethyl acetal (DMF-DMA) in refluxing toluene to give the dimethyl enamine **11**. Acid-catalyzed cyclocondensation of **11** with 3-aminopyrazole led to the formation of pyrazolo[1,5-*a*]pyrimidine **12**. Nitro reduction was followed by treatment of the resulting aniline **13** with *m*-tolyl isocyanate to complete the synthesis of urea **14**.

Compounds bearing a substituent at the 3-position of the pyrazolo[1,5-*a*]pyrimidine nucleus were prepared via a similar route, using 4-substituted 3-aminopyrazoles in place of 3-aminopyrazole in the cyclocondensation step. 3-Aminopyrazole derivatives that were not available from commercial sources were prepared through synthetic sequences based on the route exemplified for compound **19** in Scheme 4. *N*-Methylpyrazole was formylated according to the Vilsmaier–Haack protocol, and the resulting aldehyde **15** was reduced to the alcohol **16** using sodium borohydride. Conversion to the chloromethyl derivative

**Table 1.** KDR Inhibitory Activity of Initial Pyrazolo[1,5-*a*]pyrimidine Analogues


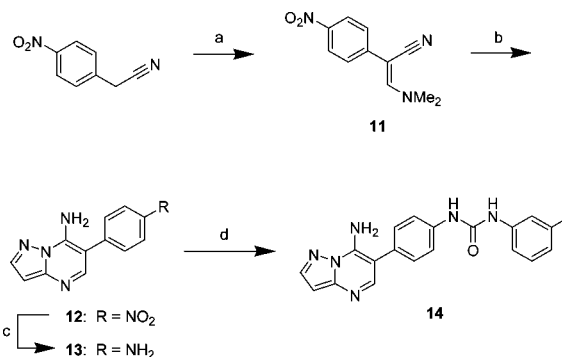
compd	X	Y	R <sub>3</sub>	R <sub>4</sub>	KDR
					(IC <sub>50</sub> , nM) <sup>a</sup>
3	Br	NH <sub>2</sub>	H	H	> 12,500
4	Br	NH <sub>2</sub>	H	OMe	> 12,500
5	Br	NH <sub>2</sub>	H	NH <sub>2</sub>	> 12,500
6	Br	NH <sub>2</sub>	H		72
7	Br	NH <sub>2</sub>	H		> 12,500
10	Br	H	H		> 12,500
14	H	NH <sub>2</sub>	H		47
23	H	NH <sub>2</sub>		H	6600
24	H	NH <sub>2</sub>	H		10,000

<sup>a</sup> Each IC<sub>50</sub> determination was performed with seven concentrations, and each assay point was determined in duplicate.

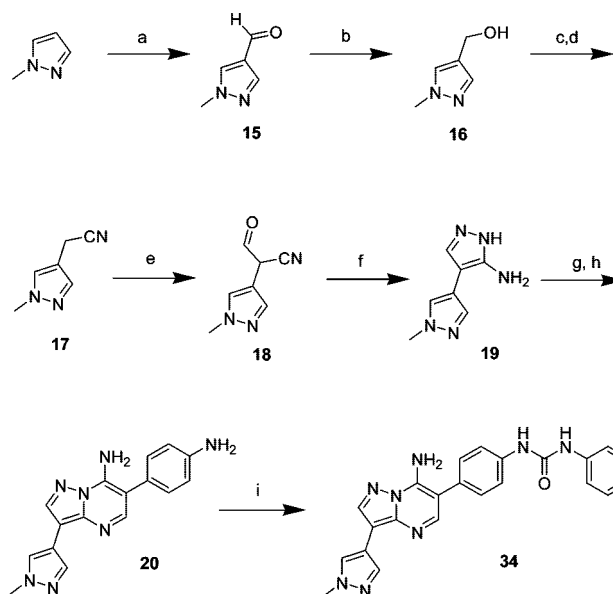
**Scheme 2.** Synthesis of 7-*des*-Aminopyrazolo[1,5-*a*]pyrimidine Urea **10**<sup>a</sup>

<sup>a</sup> Conditions: (a) concentrated HCl, EtOH, reflux, 93%; (b) HNO<sub>3</sub>, H<sub>2</sub>SO<sub>4</sub>, -20 °C to room temp; (c) Fe<sup>0</sup>, NH<sub>4</sub>Cl, THF, EtOH, H<sub>2</sub>O, 80 °C, 34% (two-step yield); (d) *m*-tolyl isocyanate, DMF, -20 °C to room temp, 51%.

by treatment with thionyl chloride was followed by displacement of the chloride with sodium cyanide to give acetonitrile derivative **17**. This compound was then formylated under basic conditions, and the resulting oxopropionitrile derivative **18** was condensed with hydrazine to give 4-substituted 3-aminopyrazole **19**. Cyclocondensation with compound **11** as previously described gave the 7-aminopyrazolo[1,5-*a*]pyrimidine bearing the *N*-methylpyrazole substituent in the 3-position. Reduction of the nitro group to the aniline **20** followed by treatment with isocyanate provided the urea **34**. Compounds **29**–**33** (Table 2) bearing substituents in the 3-position were prepared from

**Scheme 3.** Synthesis of 7-Aminopyrazolo[1,5-*a*]pyrimidine Urea **14** from 4-Nitrophenylacetonitrile<sup>a</sup>

<sup>a</sup> Conditions: (a) CH(OCH<sub>3</sub>)<sub>2</sub>N(CH<sub>3</sub>)<sub>2</sub>, toluene, reflux, 95%; (b) 3-aminopyrazole, concentrated HCl, EtOH, reflux, 86%; (c) H<sub>2</sub> (1 atm), Pd/C, MeOH, 94%; (d) *m*-tolyl isocyanate, DMF, -20 °C to room temp, 75%.

**Scheme 4.** Synthesis of C3-Substituted 7-Aminopyrazolo[1,5-*a*]pyrimidine Urea **34**<sup>a</sup>

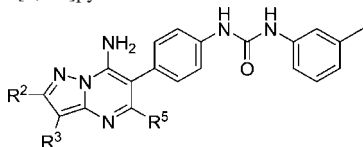
<sup>a</sup> Conditions: (a) POCl<sub>3</sub>, DMF, 0–70 °C, 79%; (b) NaBH<sub>4</sub>, MeOH, 92%; (c) SOCl<sub>2</sub>, CHCl<sub>3</sub>, reflux; (d) NaCN, DMSO, 43% (two-steps); (e) HCO<sub>2</sub>Et, NaH, catalytic EtOH, toluene; (f) H<sub>2</sub>NNH<sub>2</sub>·H<sub>2</sub>O, concentrated HCl, EtOH, reflux, 45% (two steps); (g) **11**, concentrated HCl, EtOH, reflux, 79%; (h) SnCl<sub>2</sub>, HCl, 0 °C to room temp, 80%; (i) *m*-tolyl isocyanate, DMF, -20 °C to room temp, 80%.

commercially available acetonitrile derivatives, as shown for the conversion of **17** to **20** in Scheme 4. Compounds **26** and **27** (Table 2), which contain substituents at the 2-position, were prepared from 3-amino-5-methylpyrazole and 3-amino-5-phenylpyrazole, and these starting materials were synthesized according to published procedures.<sup>31</sup>

Compound **28** (Table 2), which bears a methyl group at the 5-position of the bicyclic core, was prepared by substituting dimethylacetamide-dimethyl acetal for DMF-DMA when forming the cyanoenamine (Scheme 5). Compounds **38**–**40** incorporating an amide substituent in the 3-position of the pyrazolo[1,5-*a*]pyrimidine ring were prepared by saponification of ester **36** followed by EDCI-mediated coupling of the resulting acid **37** with various amines (Scheme 6).

## Biology

Compounds were assayed against a panel of receptor tyrosine kinases that included a KDR assay run in the presence of 1

**Table 2.** Substitutions at the 2, 3, and 5 Positions of the 7-Aminopyrazolo[1,5-*a*]pyrimidines


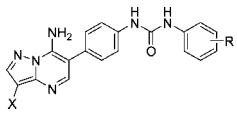
compd	R <sup>2</sup>	R <sup>3</sup>	R <sup>5</sup>	KDR (IC <sub>50</sub> , nM) <sup>a</sup>	KDR (cell) (IC <sub>50</sub> , nM) <sup>b</sup>
<b>14</b>	H	H	H	47	70
<b>6</b>	H	Br	H	72	86
<b>25</b>	H	Ph	H	22	17
<b>26</b>	CH <sub>3</sub>	H	H	3500	--
<b>27</b>	Ph	H	H	> 12,500	--
<b>28</b>	H	H	CH <sub>3</sub>	39	250
<b>29</b>	H		H	15	49
<b>30</b>	H		H	11	22
<b>31</b>	H		H	16	33
<b>32</b>	H		H	17	21
<b>33</b>	H		H	9	7
<b>34</b>	H		H	4	1
<b>35</b>	H	CN	H	930	--
<b>36</b>	H	COOEt	H	25	220
<b>37</b>	H	COOH	H	2000	--
<b>38</b>	H	CONHMe	H	100	--
<b>39</b>	H		H	790	--
<b>40</b>	H		H	500	--

<sup>a</sup> Each IC<sub>50</sub> determination was performed with seven concentrations, and each assay point was determined in duplicate. <sup>b</sup> Each cellular IC<sub>50</sub> determination was performed with five concentrations, and each assay point was determined in duplicate.

mM ATP, which is reportedly a physiologically relevant concentration.<sup>32</sup> Active compounds were then further characterized using a cellular KDR assay, and compounds showing promise in that assay progressed to in vivo studies (vide infra).

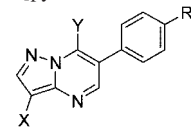
Compound **6** was prepared as the initial compound in the series and was found to be a nanomolar inhibitor of KDR (Table 1). Compound **10**, an analogue lacking the 7-amino group, was inactive, a finding consistent with the participation of this group in the hinge-binding motif proposed in Figure 2. Removal of the 3-bromo substituent of **6** to give **14** provided a roughly equipotent compound and suggested that this position might be amenable to substitution.

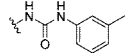
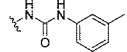
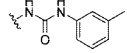
Consistent with the thienopyrimidine and isoindolinone urea series,<sup>22,23</sup> the 4-diphenylurea substituent in the 6-position was

**Table 3.** Substitutions at the Terminal Benzene Ring of the *N,N'*-Diarylureas


compd	X	R	KDR (IC <sub>50</sub> , nM) <sup>a</sup>	KDR (cell) (IC <sub>50</sub> , nM) <sup>b</sup>
<b>6</b>	Br	3-CH <sub>3</sub>	72	86
<b>6a</b>	Br	2-CH <sub>3</sub>	> 12500	
<b>6b</b>	Br	4-CH <sub>3</sub>	810	
<b>6c</b>	Br	H	1600	
<b>14</b>	H	3-CH <sub>3</sub>	47	70
<b>14a</b>	H	3-CF <sub>3</sub>	9	35
<b>14b</b>	H	3-Cl	44	
<b>14c</b>	H	2-F, 5-CH <sub>3</sub>	74	
<b>14d</b>	H	2-F, 5-CF <sub>3</sub>	14	70

<sup>a</sup> Each IC<sub>50</sub> determination was performed with seven concentrations, and each assay point was determined in duplicate. <sup>b</sup> Each cellular IC<sub>50</sub> determination was performed with five concentrations, and each assay point was determined in duplicate.

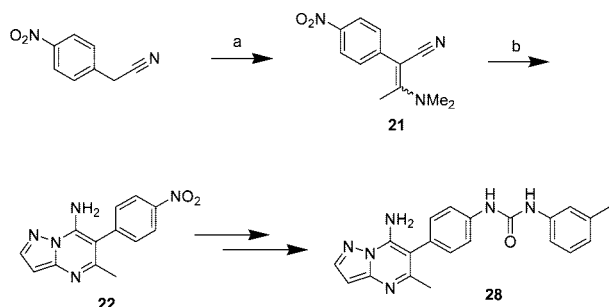
**Table 4.** Comparison of the SAR of 7-Amino- and 7-*des*-Aminopyrazolo[1,5-*a*]pyrimidine KDR Inhibitors


compd	X	Y	KDR	
			R	IC <sub>50</sub> (nM) <sup>a</sup>
<b>30</b>		NH <sub>2</sub>		11
<b>6</b>	Br	NH <sub>2</sub>		72
<b>10</b>	Br	H		> 12,500
<b>41</b>	Br	H	OMe	> 12,500
<b>42</b>		NH <sub>2</sub>	OMe	6100
<b>43<sup>b</sup></b>		H	OMe	185

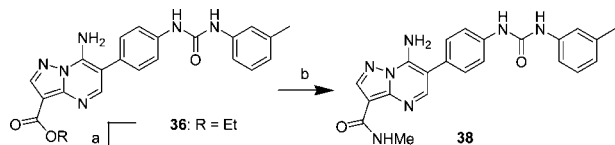
<sup>a</sup> Each IC<sub>50</sub> determination was performed with seven concentrations, and each assay point was determined in duplicate. <sup>b</sup> Compound reported in ref 34.

essential for potency in this series, as evidenced by the loss of potency shown for non-ureas **3–5** when compared to urea **6** (Table 1). Replacement of the diphenylurea of **6** with a benzamide (**7**) was also not tolerated, consistent with our model suggesting that both of the N–H moieties of the urea form hydrogen bonds to the enzyme (vide infra). Likewise, thiourea **24** demonstrated substantially diminished potency compared to the analogous urea **14**, and the meta-linked diphenylurea (**23**) also led to potency loss.

Substitution about the pyrazolopyrimidine core generated a distinct SAR (Table 2). Addition of a methyl or phenyl group in the 2-position (**26**, **27**) led to a loss of potency, consistent with the hypothesis that N-1 is acting as a hinge binder. Incorporation of a methyl group in the 5-position (**28**) was tolerated, although this led to diminished potency in the KDR cellular assay in comparison with compound **14**, which lacks this substituent. A variety of substitutions at the 3-position were tolerated, and in many cases these compounds exhibited

**Scheme 5.** Synthesis of C5-Substituted 7-Aminopyrazolo[1,5-*a*]pyrimidine **28**<sup>a</sup>


<sup>a</sup> Conditions: (a)  $\text{CH}_3\text{C}(\text{OCH}_3)_2\text{N}(\text{CH}_3)_2$ , toluene, reflux, 76%; (b) 3-aminopyrazole, concentrated HCl, EtOH, reflux, 46%.

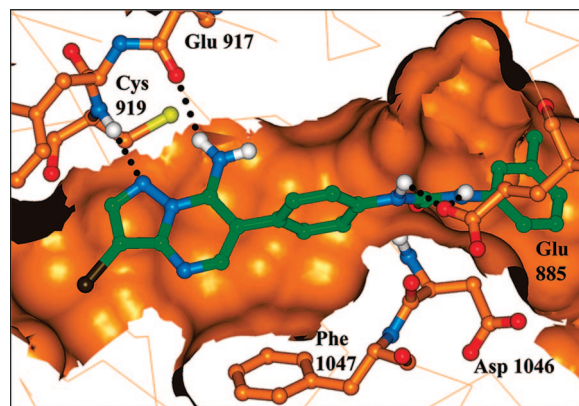
**Scheme 6.** Synthesis of Compounds **36–38**<sup>a</sup>


<sup>a</sup> Conditions: (a) LiOH, H<sub>2</sub>O, THF, MeOH, 70 °C 84%; (b) MeNH<sub>2</sub>·HCl, EDCI, HOBt, NMM, DMF, 56%.

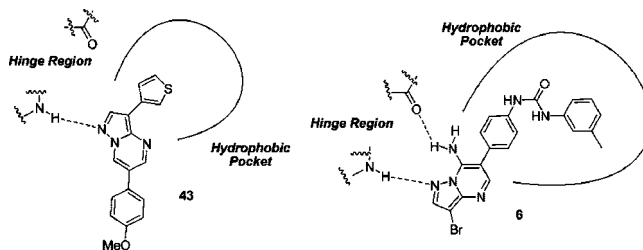
improved potency. In general, aryl, heteroaryl, and alkyl groups were favored over more polar groups. Both the 2- and 3-thiophene isomers **29** and **30** were roughly equipotent and were not significantly different from the phenyl analogue **25**. Other hydrophobic groups in the 3-position, including the smaller cyclopropyl (**31**) and larger methylenedioxyphenyl (**32**), also showed potency in the 15–25 nM range in the KDR enzyme assay. The most potent compounds in the KDR cellular assay incorporated nitrogen heterocycles in the 3-position, including 3-pyridine **33** and *N*-methylpyrazole **34**. These compounds exhibited cellular IC<sub>50</sub> values in the single-digit nanomolar range. Compounds such as nitrile **35**, acid **37**, and amides **38–40**, which bear polar substituents in the 3-position, were considerably weaker inhibitors, although the ester **36** retained potency similar to aryl compounds such as **25**, presumably because of its somewhat more hydrophobic character.

The SAR of substitution about the terminal ring of the urea was similar to that observed for the thienopyrimidine urea, isoindolinone urea, and aminoindazole series studied previously. Substitution at the 3-position was required for optimal potency, as evidenced by the strongly enhanced potency of the 3-methyl analogue **6** when compared with the 2- and 4-methyl compounds **6a** and **6b** and the unsubstituted phenyl analogue **6c** (Table 3). Further exploration of *des*-bromo compounds incorporating a 3-substituent on the terminal phenyl ring revealed that the trifluoromethyl group in compounds **14a** and **14d** was preferred over the methyl group in compounds **14** and **14c**. The 3-chloro analogue **14b** was equipotent with the methyl analogue **14**.

A plausible model of the binding mode of **6** in the active site of KDR was prepared using a method previously reported and is shown in Figure 3.<sup>22</sup> The urea portion of the inhibitor was docked as reported for another urea-based inhibitor<sup>33</sup> with hydrogen bonds between the inhibitor carbonyl and the Asp 1045 backbone N–H and between the inhibitor urea N–H groups and the side chain carboxylate of Glu 885. The pyrazolopyrimidine ring system fit well into the canonical adenosine-binding portion of the ATP-binding site, with hydrogen bonding interactions occurring between the 7-amino



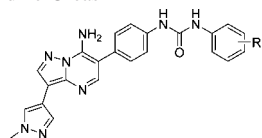
**Figure 3.** Model of compound **6** bound to KDR kinase. Hydrogen bonds in black are shown between the urea and Glu 885 carboxylate, between the exocyclic amine and Glu 917 backbone carbonyl, and between the ring nitrogen and Cys 919 N–H. Also in thick bond are residues Asp 1046–Phe 1047 of the “DFG” motif in the “inactive” conformation (“DFG-out”).



**Figure 4.** Comparison of proposed binding modes for compounds **43**<sup>34</sup> and **6**.

group and the backbone carbonyl of Glu 917 and between the pyrazolo ring nitrogen and the backbone N–H of Cys 919. This is supported by the observation that *des*-amino compound **10**, an analogue of **6** that lacks a 7-amino group, does not inhibit KDR at measured concentrations. Consistent with the observed SAR for compounds **26** and **27**, there does not appear to be room for substitution at C-2 of the pyrazolo ring.

Researchers at Merck have also described a series of pyrazolo[1,5-*a*]pyrimidines as inhibitors of KDR, including compound **43** (Table 4).<sup>30,34</sup> In order to establish whether these 7-amino pyrazolo[1,5-*a*]pyrimidines are binding in the same fashion as the previously reported compounds, hybrid compounds incorporating features of both the Abbott compounds reported in this paper and compounds from the Merck series were prepared. As shown in Table 4, it appears that these two series of compounds must be binding in distinctly different fashions with the enzyme. Introduction of a 7-amino group onto compound **43** to give **42** results in a striking loss of potency. Conversely, removal of the 7-amino group from compound **6** to give compound **10** in the urea series results in loss of measurable potency. Furthermore, Merck researchers report that compounds in their series lacking an aryl or heteroaryl group in the 3-position are inactive, as shown by comparison of 3-thienyl compound **43** to the 3-bromo compound **41**. In the 7-amino series, however, 3-bromo compound **6** is roughly equipotent with 3-thienyl analogue **30**. These findings are consistent with the contrasting binding modes proposed for the two series based on homology modeling, as shown in Figure 4. Although N-1 of the pyrazolo[1,5-*a*]pyrimidine is thought to form a hydrogen bond with Cys 919 of the hinge region in both binding modes, the 7-amino inhibitor **6** appears to be “flipped” in comparison with the *des*-amino compound **43** and also forms

**Table 5.** KDR Enzymatic and Cellular Inhibitory Activity and in Vivo Oral Uterine Edema Inhibitory Activity of 4-Methylpyrazole-Substituted Pyrazolo[1,5-*a*]pyrimidine Ureas

compd	R	KDR (IC <sub>50</sub> , nM) <sup>a</sup>	KDR (cell) (IC <sub>50</sub> , nM) <sup>b</sup>	UE <sup>c</sup> (mg/kg)
<b>34</b>	3-CH <sub>3</sub>	4	1	49% @ 10 <sup>d</sup>
<b>34a</b>	3-CF <sub>3</sub>	3	0.7	ED <sub>50</sub> = 1.4 <sup>e</sup>
<b>34b</b>	3-Cl	4	8	27% @ 10 <sup>d</sup>
<b>34c</b>	2-F, 5-CF <sub>3</sub>	5	28	45% @ 10 <sup>d</sup>
<b>34d</b>	3-CF <sub>3</sub> -4-F	6	55	inactive <sup>f</sup>
<b>34e</b>	3-F	10	29	

<sup>a</sup> Each IC<sub>50</sub> determination was performed with seven concentrations, and each assay point was determined in duplicate. <sup>b</sup> Each cellular IC<sub>50</sub> determination was performed with five concentrations, and each assay point was determined in duplicate. <sup>c</sup> Estradiol-induced murine uterine edema assay. <sup>d</sup> Values are expressed as percent inhibition @ mg/kg. <sup>e</sup> ED<sub>50</sub> values in mg/kg. <sup>f</sup> "Inactive" indicates the compound provided <15% inhibition at 10 mg/kg.

a second hydrogen bond through the 7-amino group. In the 7-amino series, it is proposed that the 6-substituent occupies the hydrophobic pocket, whereas in the *des*-amino series, the 3-substituent is thought to occupy this pocket. Modeling studies and SAR both suggest that the 7-amino series is indeed binding in a distinct binding mode from the previously reported series. This result is consistent with previous reports of kinase inhibitors exhibiting multiple binding modes.<sup>35</sup>

Compounds showing potency of <100 nM in the KDR enzymatic and cellular assays were evaluated in the estradiol-induced murine uterine edema (UE) assay, an in vivo model of VEGF-induced vascular permeability.<sup>36</sup> Mice (six per group), which had been primed with pregnant mare's serum 1 and 2 days prior to the assay, were given a KDR inhibitor orally and challenged with estradiol 30 min later. Edema was assessed 2 h following estradiol administration, comparing the uterine weights of the inhibitor-treated animals to those of estradiol-treated and untreated controls.<sup>37</sup> This model requires a minimal amount of compound and provides a medium-throughput in vivo assessment of KDR inhibition following a single oral dose and was used as a screening tool to identify compounds that would progress to in vivo tumor growth inhibition assays.

In the uterine edema assay, the most potent compounds in this series bear an *N*-methylpyrazole substituent in the 3-position (Table 5). A number of compounds incorporating meta substituents on the terminal phenyl ring were single-digit nanomolar inhibitors of KDR in the enzymatic assay, although in the cellular KDR assay the methyl and trifluoromethyl compounds **34** and **34a** were found to be somewhat more potent than the chloro and fluoro compounds **34b** and **34e** or the trifluoromethyl compounds **34c,d** incorporating an additional fluoro substituent on the ring. Compound **34a**, with an ED<sub>50</sub> of 1.4 mg/kg in the uterine edema model, was the most potent compound evaluated in this series and had efficacy comparable to that observed for the best compounds in the thienopyrimidine series.<sup>22</sup> This compound also exhibited a favorable pharmacokinetic profile characterized by low plasma clearance, high exposure, a half-life of 2.2 h, and oral availability in the mouse (Table 6). Compared to *m*-tolylurea **34**, 3-trifluoromethylphenylurea **34a** showed a 6-fold reduction in clearance following iv administration (3.7 vs 0.57), as well as a dramatic enhancement in exposure following oral dosing. This improved clearance and the corresponding enhanced exposure may correlate with the boost in potency observed for compound **34a** in the uterine edema model.

The 7-aminopyrazolo[1,5-*a*]pyrimidines herein described are potent inhibitors of KDR, and they also display significant inhibition of other VEGFR and PDGFR kinase family members, as shown in Table 7. Compound **34a** is a single-digit-nanomolar inhibitor of the VEGFR kinases KDR and Flt-1 and also of the PDGFR kinases Flt-3, c-Kit, and CSF1R.<sup>38</sup>

## Conclusion

Novel 7-aminopyrazolo[1,5-*a*]pyrimidine inhibitors of VEGFR and PDGFR kinases have been discovered. These compounds display an SAR profile that is distinct from the pyrazolo[1,5-*a*]pyrimidine KDR inhibitors previously reported by other researchers. Modeling and SAR studies suggest that these compounds bind in the ATP pocket of the enzyme, with the 7-aminopyrazolo[1,5-*a*]pyrimidine core forming a bidentate hydrogen bonding interaction with the hinge region and the *N,N'*-diarylurea occupying the hydrophobic pocket. Optimal potency was obtained by incorporation of an *N,N'*-diarylurea moiety at the 6-position, with the substituents in a para orientation on the 6-phenyl ring and a small meta substituent on the terminal phenyl ring of the urea. Additional substitution at the 3-position of the pyrazolo[1,5-*a*]pyrimidine core led to compounds with enhanced activity in the cellular KDR assay, and the placement of an *N*-methylpyrazole linked through C-4 in this position provided compounds typified by **34a**, which exhibited single-digit nanomolar inhibition of KDR in both the enzymatic and cellular assays and was found to have oral efficacy in the estradiol-induced murine uterine edema assay, an in vivo model of VEGF-induced vascular permeability.

## Experimental Section

**Chemistry.** <sup>1</sup>H NMR spectra were recorded on a 300 MHz spectrometer (Nicolet QE-300 or General Electric GN-300) if not otherwise indicated, and chemical shifts are reported in parts per million (ppm,  $\delta$ ) relative to tetramethylsilane as an internal standard. Mass spectra were obtained on a Finnigan MAT SSQ700 instrument. The above structural data were obtained through the Department of Structural Chemistry, Abbott Laboratories. Elemental analyses were performed by Robertson Microlit Laboratories, Inc., Madison, NJ, or by Quantitative Technologies Inc., Whitehouse, NJ, and the results indicated by elemental symbols are within  $\pm 0.4\%$  of theoretical values unless otherwise indicated. Preparative column chromatography was performed using silica gel 60 (E. Merck, 230–400 mesh) or, when indicated, using an Analogix IntelliFlash 280 chromatographic purification system and Analogix prefilled silica gel cartridges as described.

**3-Bromo-6-phenylpyrazolo[1,5-*a*]pyrimidin-7-amine (3).** 3-Amino-4-bromopyrazole (4.00 g, 24.7 mmol), 3-oxo-2-phenylpropanenitrile (3.60 g, 24.8 mmol), and concentrated HCl (8 mL) were combined in EtOH (150 mL). The mixture was heated to reflux for 16 h, then cooled to room temperature. The mixture was concentrated to dryness on a rotary evaporator, and the residue was dissolved in H<sub>2</sub>O (100 mL). An amount of 1 N NaOH was added until the mixture reached pH 6, and the resulting white solid was collected by filtration, rinsing with H<sub>2</sub>O, to give **3** (6.17 g, 86%). <sup>1</sup>H NMR (300 MHz, DMSO-*d*<sub>6</sub>)  $\delta$  8.29 (s, 1H), 8.17 (s, 1H), 7.70 (s, 2H), 7.48–7.54 (m, 4H), 7.37–7.45 (m, 1H); MS (ESI) *m/z* 288.8, 290.8 [M + H]<sup>+</sup>. Anal. (C<sub>12</sub>H<sub>9</sub>BrN<sub>4</sub>·0.1EtOH) C, H, N.

**6-(4-Aminophenyl)-3-bromopyrazolo[1,5-*a*]pyrimidin-7-amine (5).** Compound **3** (5.75 g, 19.9 mmol) was dissolved in concentrated H<sub>2</sub>SO<sub>4</sub> (70 mL), and the solution was chilled in a –20 °C cooling bath. A solution of concentrated HNO<sub>3</sub> (1.25 mL, 20 mmol) in concentrated H<sub>2</sub>SO<sub>4</sub> (5 mL) was added dropwise, and the mixture was allowed to warm slowly to room temperature and stirred for 2 h. The mixture was then poured carefully over ice (800 g) and adjusted to pH 6 by the addition of 5 N NaOH. A yellow precipitate formed and was collected by filtration, providing a crude nitration

**Table 6.** Pharmacokinetic Data for Pyrazolo[1,5-*a*]pyrimidine Ureas **34** and **34a**<sup>a</sup>

compd	iv <sup>b</sup>				po <sup>c</sup>		
	<i>t</i> <sub>1/2</sub> (h)	Cl (mL/(min·kg))	AUC (μg·h/mL)	V <sub>d</sub> (L/kg)	C <sub>max</sub> (μM)	AUC (μg·h/mL)	F (%)
<b>34</b>	0.25	3.7	1.8	1.4	0.36	0.81	14
<b>34a</b>	2.2	0.57	10.6	1.8	5.7	41.0	~100

<sup>a</sup> Mouse pharmacokinetics. <sup>b</sup> Dosed at 3 mg/kg in a vehicle comprising 2.5% DMSO, 2.5% Tween-80, 25% PEG400 in PBS. <sup>c</sup> Dosed at 10 mg/kg in a vehicle comprising 2.5% EtOH, 5% Tween-80, 25% PEG400 in PBS.

**Table 7.** Kinase Inhibition Profile of Pyrazolo[1,5-*a*]pyrimidine Urea **34a**<sup>a</sup>

compd	VEGFR kinases (IC <sub>50</sub> , nM)			PDGFR kinases (IC <sub>50</sub> , nM)		
	KDR	Flt-1	FGFR	Flt-3	c-Kit	CSF-1R
<b>34a</b>	3	3	>12500	5	9	4

<sup>a</sup> Each IC<sub>50</sub> determination was performed with seven concentrations, and each assay point was determined in duplicate.

product. MS (ESI) *m/z* 334.0, 335.9 [M + H]<sup>+</sup>. This material was taken up in EtOH (200 mL), THF (80 mL), and H<sub>2</sub>O (40 mL), and the mixture was heated to 70 °C, whereupon Fe<sup>0</sup> (11.1 g, 199 mmol) and NH<sub>4</sub>Cl (1.06 g, 19.8 mmol) were added. The mixture was stirred at 70 °C overnight, then cooled to room temperature and filtered, rinsing with MeOH. The filtrate was concentrated to dryness, and the residue was partitioned between H<sub>2</sub>O (500 mL) and CH<sub>2</sub>Cl<sub>2</sub> (500 mL). The aqueous layer was further extracted with CH<sub>2</sub>Cl<sub>2</sub> (2 × 250 mL), and the combined extracts were dried (Na<sub>2</sub>SO<sub>4</sub>) and concentrated onto silica gel (50 g). The silica was placed atop a flash chromatography column and eluted with EtOAc/CH<sub>2</sub>Cl<sub>2</sub> (gradient elution 4–10% EtOAc) to give **5** as a light-orange solid (1.68 g, 28%). <sup>1</sup>H NMR (300 MHz, DMSO-*d*<sub>6</sub>) δ 8.23 (s, 1H), 8.08 (s, 1H), 7.45–7.41 (br s, 2H), 7.13 (d, *J* = 8.5 Hz, 2H), 6.68 (d, *J* = 8.5 Hz, 2H), 5.25–5.24 (br s, 2H); MS (ESI) *m/z* 303.9, 305.9 [M + H]<sup>+</sup>. Anal. (C<sub>12</sub>H<sub>10</sub>BrN<sub>5</sub>·0.2CH<sub>2</sub>Cl<sub>2</sub>) C, H, N.

**1-(4-(7-Amino-3-bromopyrazolo[1,5-*a*]pyrimidin-6-yl)phenyl)-3-*m*-tolylurea (6).** A solution of **5** (100 mg, 0.33 mmol) in DMF (1 mL) was chilled to –20 °C, and *m*-tolyl isocyanate (0.045 mL, 0.35 mmol) was added dropwise. The mixture was allowed to warm to room temperature and stirred overnight, and then H<sub>2</sub>O (20 mL) was added. The mixture was extracted with EtOAc (3 × 15 mL). The extracts were dried (Na<sub>2</sub>SO<sub>4</sub>) and concentrated. The residue was triturated with CH<sub>2</sub>Cl<sub>2</sub>, and the resulting solid was collected by filtration to give **6** (67 mg, 47%). <sup>1</sup>H NMR (300 MHz, DMSO-*d*<sub>6</sub>) δ 8.81 (s, 1H), 8.62 (s, 1H), 8.27 (s, 1H), 8.15 (s, 1H), 7.65 (s, 2H), 7.59 (d, *J* = 8.5 Hz, 2H), 7.41 (d, *J* = 8.8 Hz, 2H), 7.32 (s, 1H), 7.25 (d, *J* = 8.5 Hz, 1H), 7.17 (t, *J* = 7.8 Hz, 1H), 6.80 (d, *J* = 7.5 Hz, 1H), 2.29 (s, 3H); MS (ESI) *m/z* 436.9, 438.9 [M + H]<sup>+</sup>. Anal. (C<sub>20</sub>H<sub>17</sub>BrN<sub>6</sub>O·0.2H<sub>2</sub>O·0.1CH<sub>2</sub>Cl<sub>2</sub>) C, H, N.

**1-(4-(7-Amino-3-bromopyrazolo[1,5-*a*]pyrimidin-6-yl)phenyl)-3-*o*-tolylurea (6a).** Compound **6a** was prepared following the procedure described for **6**, substituting *o*-tolyl isocyanate for *m*-tolyl isocyanate. <sup>1</sup>H NMR (300 MHz, DMSO-*d*<sub>6</sub>) δ 9.16 (s, 1H), 8.28 (s, 1H), 8.15 (s, 1H), 7.95 (s, 1H), 7.86 (dd, *J* = 8.0, 1.2 Hz, 1H), 7.65 (s, 2H), 7.60 (d, *J* = 8.8 Hz, 2H), 7.42 (d, *J* = 8.5 Hz, 2H), 7.07–7.21 (m, 2H), 6.96 (td, *J* = 7.4, 1.2 Hz, 1H), 2.26 (s, 3H); MS (ESI) *m/z* 437.1, 439.1 [M + H]<sup>+</sup>. Anal. (C<sub>20</sub>H<sub>17</sub>BrN<sub>6</sub>O) C, H, N.

**1-(4-(7-Amino-3-bromopyrazolo[1,5-*a*]pyrimidin-6-yl)phenyl)-3-*p*-tolylurea (6b).** Compound **6b** was prepared following the procedure described for **6**, substituting *p*-tolyl isocyanate for *m*-tolyl isocyanate. <sup>1</sup>H NMR (300 MHz, DMSO-*d*<sub>6</sub>) δ 8.77 (s, 1H), 8.58 (s, 1H), 8.27 (s, 1H), 8.15 (s, 1H), 7.65 (s, 2H), 7.58 (d, *J* = 8.5 Hz, 2H), 7.40 (d, *J* = 8.8 Hz, 2H), 7.35 (d, *J* = 8.1 Hz, 2H), 7.09 (d, *J* = 8.1 Hz, 2H), 2.25 (s, 3H); MS (ESI) *m/z* 437.1, 439.1 [M + H]<sup>+</sup>. Anal. (C<sub>20</sub>H<sub>17</sub>BrN<sub>6</sub>O) C, H, N.

**1-(4-(7-Amino-3-bromopyrazolo[1,5-*a*]pyrimidin-6-yl)phenyl)-3-phenylurea (6c).** Compound **6c** was prepared following the procedure described for **6**, substituting phenyl isocyanate for *m*-tolyl isocyanate. <sup>1</sup>H NMR (300 MHz, DMSO-*d*<sub>6</sub>) δ 8.82 (s, 1H), 8.69 (s, 1H), 8.27 (s, 1H), 8.15 (s, 1H), 7.65 (s, 2H), 7.59 (d, *J* = 8.8 Hz, 2H), 7.47 (d, *J* = 7.8 Hz, 2H), 7.41 (d, *J* = 8.8 Hz, 2H), 7.29

(t, *J* = 7.5 Hz, 2H), 6.98 (t, *J* = 7.3 Hz, 1H); MS (ESI) *m/z* 423.0, 425.0 [M + H]<sup>+</sup>. Anal. (C<sub>19</sub>H<sub>15</sub>BrN<sub>6</sub>O) C, H, N.

***N*-(4-(7-Amino-3-bromopyrazolo[1,5-*a*]pyrimidin-6-yl)phenyl)-benzamide (7).** A solution of **5** (100 mg, 0.33 mmol), benzoic acid (41 mg, 0.33 mmol), EDCI (78 mg, 0.41 mmol), HOBt (54 mg, 0.40 mmol), and *N*-methylmorpholine (0.18 mL, 1.5 mmol) in DMF (2 mL) was stirred overnight at room temperature, then diluted with H<sub>2</sub>O (50 mL). The mixture was extracted with EtOAc (3 × 25 mL), and the organic layers were dried (Na<sub>2</sub>SO<sub>4</sub>) and concentrated to dryness. The residue was triturated with CH<sub>2</sub>Cl<sub>2</sub> and the resulting solid was collected by filtration, rinsing with CH<sub>2</sub>Cl<sub>2</sub>, to give **7** as an off-white solid (80 mg, 60%). <sup>1</sup>H NMR (300 MHz, DMSO-*d*<sub>6</sub>) δ 10.38 (s, 1H), 8.28 (s, 1H), 8.18 (s, 1H), 7.91–8.01 (m, 4H), 7.70 (br s, 2H), 7.47–7.63 (m, 5H); MS (ESI) *m/z* 408.0, 410.0 [M + H]<sup>+</sup>. Anal. (C<sub>19</sub>H<sub>15</sub>BrN<sub>6</sub>O·0.3H<sub>2</sub>O) C, H, N.

**3-Bromo-6-phenylpyrazolo[1,5-*a*]pyrimidine (8).** A mixture 2-phenylmalonaldehyde (500 mg, 3.4 mmol), 3-amino-4-bromopyrazole (544 mg, 3.4 mmol), and concentrated HCl (1 mL, 12 mmol) in EtOH (20 mL) was heated to reflux for 2 h. The mixture was concentrated in vacuo to remove the EtOH, and the resulting residue was dissolved in H<sub>2</sub>O (100 mL). The solution was adjusted to basic pH with 1 N NaOH and the resulting solid was collected by filtration to give **8** (860 mg, 93%). <sup>1</sup>H NMR (300 MHz, DMSO-*d*<sub>6</sub>) δ 9.52 (d, *J* = 2.4 Hz, 1H), 9.03 (d, *J* = 2.0 Hz, 1H), 8.42 (s, 1H), 7.84–7.89 (m, 2H), 7.51–7.58 (m, 2H), 7.43–7.50 (m, 1H); MS (ESI) *m/z* 273.9, 275.9 [M + H]<sup>+</sup>.

**4-(3-Bromopyrazolo[1,5-*a*]pyrimidin-6-yl)phenylamine (9).** To a solution of **8** (500 mg, 1.82 mmol) in concentrated H<sub>2</sub>SO<sub>4</sub> (3 mL) at –20 °C was added dropwise concentrated HNO<sub>3</sub> (0.1 mL, 1.6 mmol). The mixture was allowed to warm to room temperature and stirred for 2 h. The mixture was poured over ice (50 g) and stirred until the ice had melted. The resulting solid was collected by filtration, then partitioned between 1 N NaOH (100 mL) and CH<sub>2</sub>Cl<sub>2</sub> (100 mL), and the aqueous layer was extracted with CH<sub>2</sub>Cl<sub>2</sub> (2 × 100 mL). The organic layers were dried (Na<sub>2</sub>SO<sub>4</sub>) and concentrated to give a mixture of nitration products in which the desired para isomer predominated. This crude solid was taken up in EtOH (40 mL), THF (16 mL), and H<sub>2</sub>O (8 mL) and the mixture was heated to 75 °C. Fe<sup>0</sup> (700 mg, 12.5 mmol) and NH<sub>4</sub>Cl (106 mg, 1.98 mmol) were added, and the mixture was kept at 75 °C for 16 h. TLC (25% EtOAc/hexanes) shows that the reaction is complete. The hot mixture was filtered through a pad of Celite, rinsing with copious amounts of MeOH, and the filtrate was concentrated in vacuo. The residue was partitioned between CH<sub>2</sub>Cl<sub>2</sub> (100 mL) and H<sub>2</sub>O (200 mL), and the aqueous layer was extracted with CH<sub>2</sub>Cl<sub>2</sub> (2 × 100 mL). The organic layers were dried (Na<sub>2</sub>SO<sub>4</sub>) and concentrated to give a crude solid, which was purified by flash chromatography (4% EtOAc in CH<sub>2</sub>Cl<sub>2</sub>) to give **9** as a pale-yellow solid (180 mg, 34%). <sup>1</sup>H NMR (300 MHz, DMSO-*d*<sub>6</sub>) δ 9.27 (d, *J* = 2.0 Hz, 1H), 8.93 (d, *J* = 2.0 Hz, 1H), 8.32 (s, 1H), 7.52 (d, *J* = 8.5 Hz, 2H), 6.68 (d, *J* = 8.5 Hz, 2H), 5.41 (s, 2H); MS (ESI) *m/z* 288.9, 290.8 [M + H]<sup>+</sup>.

**1-[4-(3-Bromopyrazolo[1,5-*a*]pyrimidin-6-yl)phenyl]-3-*m*-tolylurea (10).** Compound **10** was prepared from **9** following the procedure described for the synthesis of **6**. <sup>1</sup>H NMR (300 MHz, DMSO-*d*<sub>6</sub>) δ 9.46 (d, *J* = 2.0 Hz, 1H), 9.02 (d, *J* = 2.0 Hz, 1H), 8.92 (s, 1H), 8.71 (s, 1H), 8.39 (s, 1H), 7.80 (d, *J* = 8.8 Hz, 2H), 7.62 (d, *J* = 8.8 Hz, 2H), 7.32 (s, 1H), 7.25 (d, *J* = 9.2 Hz, 1H), 7.17 (t, *J* = 7.6 Hz, 1H), 6.80 (d, *J* = 7.5 Hz, 1H), 2.29 (s, 3H); MS (ESI) *m/z* 422.0, 423.7 [M + H]<sup>+</sup>. Anal. (C<sub>20</sub>H<sub>16</sub>BrN<sub>5</sub>O) C, H, N.

**3-Dimethylamino-2-(4-nitrophenyl)acrylonitrile (11).** To a solution of 4-nitrophenylacetonitrile (10 g, 62 mmol) in toluene (400 mL) was added dimethylformamide-dimethyl acetal (25.0 mL, 188 mmol). The mixture was heated to reflux for 16 h and then concentrated to dryness in vacuo. The residue was purified by flash chromatography, eluting with  $\text{CH}_2\text{Cl}_2$  to give **11** as a bright-yellow solid (12.7 g, 95%).  $^1\text{H}$  NMR (300 MHz,  $\text{DMSO}-d_6$ )  $\delta$  8.13 (d,  $J$  = 9.2 Hz, 2H), 7.87 (s, 1H), 7.53 (d,  $J$  = 9.2 Hz, 2H), 3.29 (s, 6H); MS (ESI)  $m/z$  218.0  $[\text{M} + \text{H}]^+$ , 124.1 (base).

**6-(4-Nitrophenyl)pyrazolo[1,5-*a*]pyrimidin-7-ylamine (12).** A solution of **11** (500 mg, 2.3 mmol) and 3-aminopyrazole (205 mg, 2.5 mmol) in EtOH (10 mL) was treated with concentrated HCl (0.5 mL, 6 mmol), and the mixture was heated to reflux for 16 h, then cooled to room temperature. A yellow precipitate formed and was collected by filtration, rinsing with EtOH, to give the title compound as its hydrochloride salt (627 mg, 86%).  $^1\text{H}$  NMR (300 MHz,  $\text{DMSO}-d_6$ )  $\delta$  9.24 (s, 2H), 8.44 (s, 1H), 8.37 (d,  $J$  = 2.4 Hz, 1H), 8.37 (d,  $J$  = 8.8 Hz, 2H), 7.82 (d,  $J$  = 8.8 Hz, 2H), 6.63 (d,  $J$  = 2.0 Hz, 1H); MS (ESI)  $m/z$  256.0  $[\text{M} + \text{H}]^+$ .

**6-(4-Aminophenyl)pyrazolo[1,5-*a*]pyrimidin-7-ylamine (13).** A suspension of the hydrochloride salt of **12** (0.62 g, 2.1 mmol) in MeOH (20 mL) was purged with  $\text{N}_2$ , and 10% Pd/C (30 mg) was added. The mixture was placed under  $\text{H}_2$  (1 atm) for 3 h. The mixture was purged with  $\text{N}_2$  and filtered through a pad of Celite, rinsing with MeOH. The filtrate was concentrated to give the hydrochloride salt of **13** as a yellow solid (0.52 g, 94%).  $^1\text{H}$  NMR (300 MHz,  $\text{DMSO}-d_6$ )  $\delta$  8.66 (s, 2H), 8.28 (d,  $J$  = 2.4 Hz, 1H), 8.21 (s, 1H), 7.23 (d,  $J$  = 8.5 Hz, 2H), 6.83 (d,  $J$  = 8.1 Hz, 2H), 6.53 (d,  $J$  = 2.4 Hz, 1H); MS (ESI)  $m/z$  226.0  $[\text{M} + \text{H}]^+$ .

**1-[4-(7-Aminopyrazolo[1,5-*a*]pyrimidin-6-yl)phenyl]-3-m-tolylurea (14).** Compounds **14** and **14a-d** were prepared from **13** following the procedure described for the synthesis of **6**.  $^1\text{H}$  NMR (300 MHz,  $\text{DMSO}-d_6$ )  $\delta$  8.80 (s, 1H), 8.62 (s, 1H), 8.12 (d,  $J$  = 2.4 Hz, 1H), 8.10 (s, 1H), 7.58 (d,  $J$  = 8.5 Hz, 2H), 7.42 (d,  $J$  = 8.8 Hz, 2H), 7.37–7.41 (m, 2H), 7.32 (s, 1H), 7.25 (d,  $J$  = 8.5 Hz, 1H), 7.17 (t,  $J$  = 7.8 Hz, 1H), 6.80 (d,  $J$  = 7.1 Hz, 1H), 6.44 (d,  $J$  = 2.4 Hz, 1H), 2.29 (s, 3H); MS (ESI)  $m/z$  359.1  $[\text{M} + \text{H}]^+$ . Anal. ( $\text{C}_{20}\text{H}_{18}\text{N}_6\text{O}\cdot 0.2\text{H}_2\text{O}$ ) C, H, N.

**1-(4-(7-Aminopyrazolo[1,5-*a*]pyrimidin-6-yl)phenyl)-3-(3-trifluoromethyl)phenyl)urea (14a).**  $^1\text{H}$  NMR (300 MHz,  $\text{DMSO}-d_6$ )  $\delta$  9.09 (s, 1H), 8.95 (s, 1H), 8.12 (d,  $J$  = 2.0 Hz, 1H), 8.10 (s, 1H), 8.02–8.04 (m, 1H), 7.58–7.63 (m, 3H), 7.52 (t,  $J$  = 8.0 Hz, 1H), 7.43 (d,  $J$  = 8.8 Hz, 2H), 7.40 (br s, 2H), 7.32 (d,  $J$  = 7.5 Hz, 1H), 6.45 (d,  $J$  = 2.4 Hz, 1H); MS (ESI)  $m/z$  413.1  $[\text{M} + \text{H}]^+$ . Anal. ( $\text{C}_{20}\text{H}_{15}\text{F}_3\text{N}_6\text{O}\cdot 0.5\text{H}_2\text{O}$ ) C, H, N.

**1-(4-(7-Aminopyrazolo[1,5-*a*]pyrimidin-6-yl)phenyl)-3-(3-chlorophenyl)urea (14b).**  $^1\text{H}$  NMR (300 MHz,  $\text{DMSO}-d_6$ )  $\delta$  8.94 (s, 1H), 8.92 (s, 1H), 8.13 (d,  $J$  = 2.4 Hz, 1H), 8.10 (s, 1H), 7.72–7.74 (m, 1H), 7.59 (d,  $J$  = 8.8 Hz, 2H), 7.43 (d,  $J$  = 8.5 Hz, 2H), 7.40 (br s, 2H), 7.27–7.32 (m, 2H), 7.03 (ddd,  $J$  = 6.3, 2.4, 2.2 Hz, 1H), 6.45 (d,  $J$  = 2.4 Hz, 1H); MS (ESI)  $m/z$  377.0  $[\text{M} + \text{H}]^+$ . Anal. ( $\text{C}_{19}\text{H}_{15}\text{ClN}_6\text{O}\cdot 0.4\text{H}_2\text{O}$ ) C, H, N.

**1-(4-(7-Aminopyrazolo[1,5-*a*]pyrimidin-6-yl)phenyl)-3-(2-fluoro-5-methylphenyl)urea (14c).**  $^1\text{H}$  NMR (300 MHz,  $\text{DMSO}-d_6$ )  $\delta$  9.19 (s, 1H), 8.50 (d,  $J$  = 2.4 Hz, 1H), 8.13 (d,  $J$  = 2.4 Hz, 1H), 8.10 (s, 1H), 8.01 (dd,  $J$  = 8.0, 1.9 Hz, 1H), 7.58 (d,  $J$  = 8.5 Hz, 2H), 7.43 (d,  $J$  = 8.5 Hz, 2H), 7.40 (br s, 2H), 7.12 (dd,  $J$  = 11.4, 8.3 Hz, 1H), 6.78–6.84 (m, 1H), 6.45 (d,  $J$  = 2.4 Hz, 1H), 2.28 (s, 3H); MS (ESI)  $m/z$  377.2  $[\text{M} + \text{H}]^+$ . Anal. ( $\text{C}_{20}\text{H}_{17}\text{FN}_6\text{O}\cdot 1.0\text{H}_2\text{O}$ ) C, H, N.

**1-(4-(7-Aminopyrazolo[1,5-*a*]pyrimidin-6-yl)phenyl)-3-(2-fluoro-5-(trifluoromethyl)phenyl)urea (14d).**  $^1\text{H}$  NMR (300 MHz,  $\text{DMSO}-d_6$ )  $\delta$  9.31 (s, 1H), 8.93 (s, 1H), 8.64 (dd,  $J$  = 7.3, 2.2 Hz, 1H), 8.13 (d,  $J$  = 2.4 Hz, 1H), 8.10 (s, 1H), 7.60 (d, 2H), 7.51 (dd,  $J$  = 10.5, 8.5 Hz, 1H), 7.37–7.47 (m, 5H), 6.45 (d,  $J$  = 2.4 Hz, 1H); MS (ESI)  $m/z$  431.1  $[\text{M} + \text{H}]^+$ . Anal. ( $\text{C}_{20}\text{H}_{14}\text{F}_4\text{N}_6\text{O}\cdot 0.1\text{H}_2\text{O}$ ) C, H, N.

**1-Methyl-1H-pyrazole-4-carbaldehyde (15).** A 500 mL, two-necked round-bottomed flask equipped with an addition funnel, a water-cooled reflux condenser, and a magnetic stir bar was charged with DMF (35 mL). The condenser was equipped with a drying

tube filled with Drierite. The flask was then cooled in an ice bath, and  $\text{POCl}_3$  (17.0 mL, 186 mmol) was added dropwise over 10 min. The mixture was stirred for 30 min at 0 °C, followed by dropwise addition of a solution of *N*-methylpyrazole (5.0 g, 61 mmol) in DMF (12 mL) over 15 min. The ice bath was removed, and the mixture was stirred at room temperature for 16 h. The solution was then chilled to 0 °C, and saturated aqueous  $\text{NaHCO}_3$  was added until the reaction was no longer acidic. The resulting mixture was extracted with EtOAc (3  $\times$  200 mL), and the extracts were dried over  $\text{Na}_2\text{SO}_4$  and concentrated in vacuo to give **15** as a crude amber oil (5.3 g, 79%), which was judged sufficiently pure to be used in the next reaction.  $^1\text{H}$  NMR (300 MHz,  $\text{DMSO}-d_6$ )  $\delta$  9.78 (s, 1H), 8.42 (s, 1H), 7.96 (s, 1H), 3.90 (s, 3H). MS (ESI)  $m/z$  111.1  $[\text{M} + \text{H}]^+$ , 258.0.

**(1-Methyl-1H-pyrazol-4-yl)methanol (16).** A solution of compound **15** (5.6 g, 51 mmol) in MeOH (500 mL) was chilled to 0 °C, and  $\text{NaBH}_4$  (3.8 g, 100 mmol) was added portionwise over 10 min. The ice bath was removed, and the mixture was stirred for 1 h. TLC (19:1  $\text{CH}_2\text{Cl}_2/\text{MeOH}$ ,  $\text{KMnO}_4$  stain) shows that the reaction is complete. The reaction was quenched with 2 N HCl (300 mL), and the MeOH was removed by concentrating in vacuo. The resulting aqueous solution was extracted with EtOAc (3  $\times$  200 mL). The extracts were dried over  $\text{Na}_2\text{SO}_4$  and concentrated in vacuo to give **16** as an amber oil (5.2 g, 92%), which was used without further purification.  $^1\text{H}$  NMR (300 MHz,  $\text{DMSO}-d_6$ )  $\delta$  7.54 (s, 1H), 7.30 (s, 1H), 4.77 (t,  $J$  = 5.4 Hz, 1H), 4.32 (d,  $J$  = 5.4 Hz, 2H), 3.78 (s, 3H); MS (ESI)  $m/z$  113.1  $[\text{M} + \text{H}]^+$ .

**(1-Methyl-1H-pyrazol-4-yl)acetonitrile (17).** A solution of compound **16** (614 mg, 5.5 mmol) in  $\text{CHCl}_3$  (25 mL) was treated with  $\text{SOCl}_2$  (0.80 mL, 11 mmol). The mixture was heated to reflux for 3 h, then cooled to room temperature and concentrated in vacuo to give an oil that solidified upon standing. This crude chloride was then dissolved in DMSO (30 mL), the solution was treated with NaCN (1.1 g, 22 mmol), and the mixture was stirred overnight at room temperature. The mixture was diluted with  $\text{H}_2\text{O}$  (150 mL), and the mixture was extracted with EtOAc (3  $\times$  75 mL). The extracts were washed with brine and dried ( $\text{Na}_2\text{SO}_4$ ), then concentrated in vacuo. The residue was purified by flash chromatography (Analox Intelliflash, RS-12 cartridge, flow rate 30 mL/min), eluting with a gradient of 0–10% EtOAc/ $\text{CH}_2\text{Cl}_2$  over 30 min to provide **17** as an oil (284 mg, 43%).  $^1\text{H}$  NMR (300 MHz,  $\text{DMSO}-d_6$ )  $\delta$  7.69 (s, 1H), 7.37 (s, 1H), 3.80 (s, 3H), 3.78 (s, 2H); MS (ESI)  $m/z$  122.1  $[\text{M} + \text{H}]^+$ .

**1'-Methyl-2H,1'H-[4,4']bipyrazolyl-3-ylamine (19).** To a mixture of ethyl formate (1.60 mL, 19.8 mmol), NaH (60% dispersion in mineral oil, 1.16 g, 29 mmol), and EtOH (2 drops) in toluene (35 mL) at room temperature was added dropwise a solution of (1-methyl-1H-pyrazol-4-yl)acetonitrile **17** (1.17 g, 9.7 mmol) in toluene (10 mL) over 30 min. The mixture was stirred at room temperature for 6 h, then quenched with  $\text{H}_2\text{O}$  and brought to pH 4 using 1 N HCl (50 mL). The mixture was extracted with EtOAc (3  $\times$  100 mL). The combined extracts were dried ( $\text{Na}_2\text{SO}_4$ ) and concentrated to give **18** as a crude offwhite solid, which was carried forward without purification. MS (ESI)  $m/z$  150.0  $[\text{M} + \text{H}]^+$ . This material was combined with EtOH (40 mL), hydrazine monohydrate (0.95 mL, 19.6 mmol), and concentrated HCl (0.9 mL). The mixture was heated to reflux for 16 h, then cooled to room temperature and concentrated to dryness. The residue was dissolved in  $\text{H}_2\text{O}$  and neutralized by the addition of saturated aqueous  $\text{NaHCO}_3$ . The resulting mixture was extracted with EtOAc (3  $\times$  50 mL). The extracts were dried ( $\text{Na}_2\text{SO}_4$ ) and concentrated in vacuo to provide **19** as a yellow wax (0.71 g, 45%).  $^1\text{H}$  NMR (300 MHz,  $\text{DMSO}-d_6$ )  $\delta$  11.42–11.54 (br s, 1H), 7.78 (s, 1H), 7.55 (app s, 2H), 4.36–4.51 (br s, 2H), 3.81 (s, 3H); MS (ESI)  $m/z$  164.1  $[\text{M} + \text{H}]^+$ .

**6-(4-Aminophenyl)-3-(1-methyl-1H-pyrazol-4-yl)pyrazolo[1,5-*a*]pyrimidin-7-ylamine (20).** 3-(1-Methyl-1H-pyrazol-4-yl)-6-(4-nitrophenyl)pyrazolo[1,5-*a*]pyrimidin-7-amine was prepared via cyclocondensation of **11** with **19** following the procedure described for the synthesis of **12**, and the resulting nitro compound was reduced to **20** as follows: 3-(1-methyl-1H-pyrazol-4-yl)-6-(4-

nitrophenyl)pyrazolo[1,5-*a*]pyrimidin-7-amine (408 mg, 1.2 mmol) was suspended in concentrated HCl (10 mL), and mixture was chilled to 0 °C. SnCl<sub>2</sub>·2H<sub>2</sub>O (824 mg, 3.6 mmol) was added, and the mixture was stirred at room temperature for 5 h. The precipitate was collected by filtration and rinsed with a little concentrated HCl, then dissolved in H<sub>2</sub>O (1000 mL). The solution was filtered, and the filtrate was neutralized by the addition of saturated aqueous NaHCO<sub>3</sub>. The mixture was extracted with EtOAc (3 × 50 mL). The extracts were dried (Na<sub>2</sub>SO<sub>4</sub>) and concentrated to provide **20** as a yellow solid (300 mg, 80%). <sup>1</sup>H NMR (300 MHz, DMSO-*d*<sub>6</sub>) δ 8.37 (s, 1H), 8.13 (s, 1H), 8.08 (s, 1H), 7.91 (s, 1H), 7.21 (s, 2H), 7.16 (d, *J* = 8.1 Hz, 2H), 6.69 (d, *J* = 8.5 Hz, 2H), 5.22 (s, 2H), 3.88 (s, 3H); MS (ESI) *m/z* 306.1 [M + H]<sup>+</sup>.

**1-{4-[7-Amino-3-(1-methyl-1*H*-pyrazol-4-yl)pyrazolo[1,5-*a*]pyrimidin-6-yl]phenyl}-3-*m*-tolyl-urea (**34**). Compounds **34** and **34a–e** were prepared from **20** following the procedure described for the synthesis of **6**. <sup>1</sup>H NMR (300 MHz, DMSO-*d*<sub>6</sub>) δ 8.79 (s, 1H), 8.61 (s, 1H), 8.41 (s, 1H), 8.15 (s, 1H), 8.14 (s, 1H), 7.93 (d, *J* = 0.7 Hz, 1H), 7.59 (d, *J* = 8.8 Hz, 2H), 7.41–7.46 (m, 4H), 7.32 (s, 1H), 7.25 (d, *J* = 8.1 Hz, 1H), 7.17 (t, *J* = 7.8 Hz, 1H), 6.80 (d, *J* = 7.5 Hz, 1H), 3.89 (s, 3H), 2.29 (s, 3H); MS (ESI) *m/z* 439.1 [M + H]<sup>+</sup>. Anal. (C<sub>24</sub>H<sub>22</sub>N<sub>8</sub>O·0.2H<sub>2</sub>O) C, H, N.**

**1-{4-[7-Amino-3-(1-methyl-1*H*-pyrazol-4-yl)pyrazolo[1,5-*a*]pyrimidin-6-yl]phenyl}-3-(3-trifluoromethylphenyl)urea (**34a**). <sup>1</sup>H NMR (300 MHz, DMSO-*d*<sub>6</sub>) δ 9.08 (s, 1H), 8.95 (s, 1H), 8.41 (s, 1H), 8.15 (s, 2H), 8.03 (s, 1H), 7.93 (s, 1H), 7.59–7.64 (m, 3H), 7.53 (t, *J* = 7.8 Hz, 1H), 7.43–7.48 (m, 4H), 7.32 (d, *J* = 7.5 Hz, 1H), 3.89 (s, 3H); MS (ESI) *m/z* 493.1 [M + H]<sup>+</sup>. Anal. (C<sub>24</sub>H<sub>19</sub>F<sub>3</sub>N<sub>8</sub>O) C, H, N.**

**1-{4-[7-Amino-3-(1-methyl-1*H*-pyrazol-4-yl)pyrazolo[1,5-*a*]pyrimidin-6-yl]phenyl}-3-(3-chlorophenyl)urea (**34b**). <sup>1</sup>H NMR (300 MHz, DMSO-*d*<sub>6</sub>) δ 8.92 (s, 1H), 8.91 (s, 1H), 8.41 (s, 1H), 8.15 (app s, 2H), 7.93 (s, 1H), 7.72–7.75 (m, 1H), 7.60 (d, *J* = 8.8 Hz, 2H), 7.42–7.48 (m, 4H), 7.27–7.35 (m, 2H), 7.03 (dt, *J* = 6.1, 2.7 Hz, 1H), 3.89 (s, 3H); MS (ESI) *m/z* 459.1 [M + H]<sup>+</sup>. Anal. (C<sub>23</sub>H<sub>19</sub>ClN<sub>8</sub>O·0.1H<sub>2</sub>O·0.1CH<sub>2</sub>Cl<sub>2</sub>) C, H, N.**

**1-{4-[7-Amino-3-(1-methyl-1*H*-pyrazol-4-yl)pyrazolo[1,5-*a*]pyrimidin-6-yl]phenyl}-3-(2-fluoro-5-trifluoromethylphenyl)urea (**34c**). <sup>1</sup>H NMR (300 MHz, DMSO-*d*<sub>6</sub>) δ 9.32 (s, 1H), 8.94 (s, 1H), 8.65 (dd, *J* = 7.1, 2.4 Hz, 1H), 8.41 (s, 1H), 8.15 (s, 2H), 7.93 (s, 1H), 7.58–7.63 (d, *J* = 8.8 Hz, 2H), 7.37–7.56 (m, 6H), 3.86–3.92 (s, 3H); MS (ESI) *m/z* 511.2 [M + H]<sup>+</sup>. Anal. (C<sub>24</sub>H<sub>18</sub>F<sub>4</sub>N<sub>8</sub>O) C, H, N.**

**1-{4-[7-Amino-3-(1-methyl-1*H*-pyrazol-4-yl)pyrazolo[1,5-*a*]pyrimidin-6-yl]phenyl}-3-(4-fluoro-3-trifluoromethylphenyl)urea (**34d**). <sup>1</sup>H NMR (300 MHz, DMSO-*d*<sub>6</sub>) δ 9.06 (s, 1H), 8.95 (s, 1H), 8.41 (s, 1H), 8.15 (app s, 2H), 8.02 (dd, *J* = 0.6, 2.5 Hz, 1H), 7.93 (s, 1H), 7.64–7.71 (m, 1H), 7.61 (d, *J* = 8.5 Hz, 2H), 7.41–7.49 (m, 5H), 3.89 (s, 3H); MS (ESI) *m/z* 511.2 [M + H]<sup>+</sup>. Anal. (C<sub>24</sub>H<sub>18</sub>F<sub>4</sub>N<sub>8</sub>O·0.2H<sub>2</sub>O) C, H, N.**

**1-{4-[7-Amino-3-(1-methyl-1*H*-pyrazol-4-yl)pyrazolo[1,5-*a*]pyrimidin-6-yl]phenyl}-3-(3-fluorophenyl)urea (**34e**). <sup>1</sup>H NMR (300 MHz, DMSO-*d*<sub>6</sub>) δ 8.94 (s, 1H), 8.90 (s, 1H), 8.41 (s, 1H), 8.15 (app s, 2H), 7.93 (s, 1H), 7.60 (d, *J* = 8.8 Hz, 2H), 7.51 (dt, *J* = 12.0, 2.3 Hz, 1H), 7.45 (s, 2H), 7.42–7.47 (m, *J* = 8.5 Hz, 2H), 7.32 (td, *J* = 8.2, 7.0 Hz, 1H), 7.13–7.17 (m, 1H), 6.79 (td, *J* = 8.4, 2.5 Hz, 1H), 3.89 (s, 3H); MS (ESI) *m/z* 443.1 [M + H]<sup>+</sup>. Anal. (C<sub>23</sub>H<sub>19</sub>FN<sub>8</sub>O·0.1CH<sub>2</sub>Cl<sub>2</sub>) C, H, N.**

**1-{4-(7-Amino-5-methylpyrazolo[1,5-*a*]pyrimidin-6-yl)phenyl}-3-*m*-tolylurea (**28**). Compound **28** was prepared from 3-aminopyrazole and dimethylacetamide-dimethyl acetal following the same sequence described for the synthesis of **14** from 3-aminopyrazole and dimethylformamide-dimethyl acetal, substituting the nitro reduction protocol described for the synthesis of compound **20**. <sup>1</sup>H NMR (300 MHz, DMSO-*d*<sub>6</sub>) δ 8.79 (s, 1H), 8.62 (s, 1H), 8.04 (d, *J* = 2.4 Hz, 1H), 7.59 (d, *J* = 8.8 Hz, 2H), 7.32 (s, 1H), 7.21–7.28 (m, 3H), 7.17 (t, *J* = 7.6 Hz, 1H), 6.78–6.83 (m, 3H), 6.30 (d, *J* = 2.0 Hz, 1H), 2.29 (s, 3H), 2.14 (s, 3H); MS (ESI) *m/z* 373.1 [M + H]<sup>+</sup>. Anal. (C<sub>21</sub>H<sub>20</sub>N<sub>6</sub>O·0.3H<sub>2</sub>O) C, H, N.**

**7-Amino-6-[4-(3-*m*-tolylureido)phenyl]pyrazolo[1,5-*a*]pyrimidine-3-carboxylic Acid Ethyl Ester (**36**). Compound **36** was prepared from 3-aminopyrazole-4-carboxylic acid ethyl ester following the sequence described for the synthesis of **14** from 3-aminopyrazole, substituting the nitro reduction protocol described for the synthesis of **5**. <sup>1</sup>H NMR (300 MHz, DMSO-*d*<sub>6</sub>) δ 8.82 (s, 1H), 8.62 (s, 1H), 8.52 (s, 1H), 8.25 (s, 1H), 7.80 (s, 2H), 7.60 (d, *J* = 8.8 Hz, 2H), 7.42 (d, *J* = 8.5 Hz, 2H), 7.32 (s, 1H), 7.25 (d, *J* = 8.5 Hz, 1H), 7.17 (t, *J* = 7.6 Hz, 1H), 6.80 (d, *J* = 7.1 Hz, 1H), 4.27 (q, *J* = 7.1 Hz, 2H), 2.29 (s, 3H), 1.31 (t, *J* = 7.1 Hz, 3H); MS (ESI) *m/z* 431.2 [M + H]<sup>+</sup>. Anal. (C<sub>23</sub>H<sub>22</sub>N<sub>6</sub>O<sub>3</sub>·1.0DMF) C, H, N.**

**7-Amino-6-[4-(3-*m*-tolylureido)phenyl]pyrazolo[1,5-*a*]pyrimidine-3-carboxylic Acid (**37**). A mixture of compound **36** (113 mg, 0.26 mmol), 2 N aqueous LiOH (0.7 mL, 1.4 mmol), MeOH (0.5 mL), and THF (1 mL) was heated to 70 °C for 3 h, at which time TLC (19:1 CH<sub>2</sub>Cl<sub>2</sub>/MeOH) showed consumption of starting material. The mixture was concentrated to dryness, and the residue was taken up in H<sub>2</sub>O (25 mL). The solution was adjusted to pH 4 with glacial HOAc and the resulting white solid was collected by filtration, rinsing with H<sub>2</sub>O, to give **37** (88 mg, 84%). <sup>1</sup>H NMR (300 MHz, DMSO-*d*<sub>6</sub>) δ 9.26 (s, 1H), 9.06 (s, 1H), 8.42 (s, 1H), 8.18 (s, 1H), 7.67–7.79 (br s, 2H), 7.63 (d, *J* = 8.5 Hz, 2H), 7.42 (d, *J* = 8.5 Hz, 2H), 7.36 (s, 1H), 7.29 (d, *J* = 8.1 Hz, 1H), 7.16 (t, *J* = 7.8 Hz, 1H), 6.79 (d, *J* = 7.5 Hz, 1H), 2.29 (s, 3H); MS (ESI) *m/z* 403.1 [M + H]<sup>+</sup>. Anal. (C<sub>21</sub>H<sub>18</sub>N<sub>6</sub>O<sub>3</sub>·2.7H<sub>2</sub>O) C, N, H calcd 5.23, found 4.66.**

**7-Amino-6-[4-(3-*m*-tolylureido)phenyl]pyrazolo[1,5-*a*]pyrimidine-3-carboxylic Acid Methylamide (**38**). A mixture of compound **37** (25 mg, 0.062 mmol), MeNH<sub>2</sub>·HCl (9 mg, 0.13 mmol), EDCI (36 mg, 0.19 mmol), HOBt (25 mg, 0.18 mmol), and *N*-methylmorpholine (0.07 mL, 0.63 mmol) in DMF (0.3 mL) was stirred for 16 h at room temperature. The mixture was diluted with H<sub>2</sub>O (10 mL) and extracted with EtOAc (3 × 10 mL). The extracts were dried (Na<sub>2</sub>SO<sub>4</sub>) and concentrated in vacuo, and the crude residue was triturated with CH<sub>2</sub>Cl<sub>2</sub>, yielding a solid that was collected by filtration to provide **38** (14 mg, 56%). <sup>1</sup>H NMR (300 MHz, DMSO-*d*<sub>6</sub>) δ 8.82 (s, 1H), 8.62 (s, 1H), 8.45 (s, 1H), 8.22 (s, 1H), 7.99 (q, *J* = 4.5 Hz, 1H), 7.90 (s, 2H), 7.60 (d, *J* = 8.8 Hz, 2H), 7.42 (d, *J* = 8.5 Hz, 2H), 7.31 (s, 1H), 7.25 (d, *J* = 8.5 Hz, 1H), 7.17 (t, *J* = 7.8 Hz, 1H), 6.80 (d, *J* = 7.1 Hz, 1H), 2.88 (d, *J* = 4.7 Hz, 3H), 2.29 (s, 3H); MS (ESI) *m/z* 416.2 [M + H]<sup>+</sup>. Anal. (C<sub>22</sub>H<sub>21</sub>N<sub>7</sub>O<sub>2</sub>·1.5H<sub>2</sub>O) C, H, N.**

**Homogeneous Time-Resolved Fluorescence (HTRF) Assays of Receptor Tyrosine Kinases (KDR, CSIR, cKIT, FLT1, FLT3).** Assays were performed in a total of 40 μL in 96-well Costar black half-volume plates using HTRF technology.<sup>39</sup> Peptide substrate (Biotin-Ahx-AEEEEYFLFA-amide) at 4 μM, 1 mM ATP, enzyme, and inhibitors were incubated for 1 h at ambient temperature in 50 mM Hepes/NaOH, pH 7.5, 10 mM MgCl<sub>2</sub>, 2 mM MnCl<sub>2</sub>, 2.5 mM DTT, 0.1 mM orthovanadate, and 0.01% BSA. Inhibitors were added to the wells at final concentrations of 3.2 nM to 50 μM with 5% DMSO added as cosolvent. The reactions were stopped with 10 μL/well 0.5 M EDTA and then 75 μL buffer containing streptavidin–allophycocyanin (Prozyme, 1.1 μg/mL), and PT66 antibody europium cryptate (Cis-Bio, 0.1 μg/mL) was added to each well. The plates were read from 1 to 4 h after addition of the detection reagents, and the time-resolved fluorescence (665–615 ratio) was measured using a Packard Discovery instrument. The amount of each tyrosine kinase added to the wells was calibrated to give a control (no inhibitor) to background (prequenched with EDTA) ratio of 10–15 and was shown to be in the low nanomolar concentration range for each kinase. The inhibition of each well was calculated using the control and background readings for that plate. Inhibition constants are the mean of two determinations performed with seven concentrations of the test compounds.

**Enzyme-Linked Immunosorbent Assay (ELISA) of KDR Cellular Phosphorylation.** NIH3T3 cells stably transfected with full length human KDR (VEGFR2) were maintained in DMEM medium with 10% fetal bovine serum and 500 μg/mL Geneticin. KDR cells were plated at 20 000 cells/well into duplicate 96-well tissue culture plates and cultured overnight in an incubator at 37 °C with 5%

CO<sub>2</sub> and 80% humidity. The growth medium was replaced with serum-free growth medium for 2 h prior to compound addition. Compounds in DMSO were diluted in serum-free growth medium (final DMSO concentration of 1%) and added to cells for 20 min prior to stimulation for 10 min with VEGF (50 ng/mL). Cells were lysed by addition of RIPA buffer (50 mM Tris-HCl (pH 7.4), 1% IGEPAL, 150 mM NaCl, 1 mM EDTA, and 0.25% sodium deoxycholate) containing protease inhibitors (Sigma cocktail), NaF (1 mM), and Na<sub>3</sub>VO<sub>4</sub> (1 mM) and placed on a microtiter plate shaker for 10 min. The lysates from duplicate wells were combined, and 170  $\mu$ L of the combined lysate was added to the KDR ELISA plate. The KDR ELISA plate was prepared by adding anti-VEGFR2 antibody (1  $\mu$ g/well, R&D Systems) to an unblocked plate and incubated overnight at 4 °C. The plate was then blocked for at least 1 h with 200  $\mu$ L/well of 5% dry milk in PBS. The plate was washed two times with PBS containing 0.1% Tween 20 (PBST) before addition of the cell lysates. Cell lysates were incubated in the KDR ELISA plate with constant shaking on a microtiter plate shaker for 2 h at room temperature. The cell lysate was then removed and the plate washed five times with PBST. Detection of phospho-KDR was performed using a 1:2000 dilution of biotinylated 4G10 antiphosphotyrosine (UBI, Lake Placid, NY), incubated with constant shaking for 1.5 h at room temperature, and washed five times with PBST, and for detection a 1:2000 dilution of streptavidin-HRP (UBI, Lake Placid, NY) was added and incubated with constant shaking for 1 h at room temperature. The wells were then washed five times with PBST, and K-Blue HRP ELISA substrate (Neogen) was added to each well. Development time was monitored at 650 nm in a SpectraMax Plus plate reader until 0.4–0.5 absorbance units were obtained (approximately 10 min) in the VEGF only wells. Phosphoric acid (1 M) was added to stop the reaction, and the plate was read at 450 nm. Percent inhibition was calculated using the VEGF only wells as 100% controls and wells containing 5  $\mu$ M pan-kinase inhibitor as 0% controls (no VEGF wells were used to monitor endogenous phosphorylation state of the cells). IC<sub>50</sub> values were calculated by nonlinear regression analysis of the concentration–response curve. Each IC<sub>50</sub> determination was performed with five concentrations and each assay point determined in duplicate.

**Estradiol-Induced Murine UE Assay.** The 12 week old balb/c female mice (Taconic, Germantown, NY) were pretreated with 10 units of pregnant mare's serum gonadotropin (PMSG, Calbiochem) intraperitoneally (ip) administered 72 and 24 h prior to estradiol. Mice were randomized the day of the experiment. Test compounds were formulated in a variety of vehicles and administered po 30 min prior to stimulation with an ip injection of water soluble 17 $\beta$ -estradiol (20–25  $\mu$ g/mouse). Animals were sacrificed and uteri removed 2.5 h following estradiol stimulation by cutting just proximal to the cervix and at the fallopian tubes. After the removal of fat and connective tissue, uteri were weighed, squeezed between filter paper to remove fluid, and weighed again. The difference between wet and blotted weights represented the fluid content of the uterus. Compound-treated groups were compared to vehicle-treated groups after subtracting the background water content of unstimulated uteri. Experimental group size was five or six.

**Mouse PK Analysis.** Male CD-1 mice weighing 26–30 g (Charles River Laboratories) were dosed intravenously via the tail vein or orally by gavage with a metal feeder tube. Dosing solutions were prepared in 2.5% ethanol, 2.5% DMSO, 5% Tween-80, 25% PEG 400, and pH 7.4 PBS for a dosing volume of 10 mL/kg. Blood samples were collected with a heparinized syringe by cardiac puncture following CO<sub>2</sub> asphyxiation at specified times. Plasma samples were aliquoted into 96-well plates, and proteins were precipitated using acidified methanol. Supernatants were stored at –20 °C. Sample analyses were performed by LC–MS using a Shimadzu 10A-VP chromatography system with a Waters YMC-AQ 5 cm column. The mobile phase consisted of 45% acetonitrile and 0.1% acetic acid in water, and the flow rate was 0.4 mL/min. Mass detection was accomplished with an ESI equipped LCQ-Duo by ThermoFinnigan. External standards were prepared from spiked

control plasma and used to generate a response factor for every study. Limits of detection were between 20 and 50 nM.

**Acknowledgment.** We thank the Department of Structural Chemistry, Abbott Laboratories, for recording the NMR and MS spectral data.

**Supporting Information Available:** Synthesis and spectral data for compounds **2**, **4**, **23–27**, **29–33**, **35**, **39**, **40**, and **42**. This material is available free of charge via the Internet at <http://pubs.acs.org>.

## References

- (1) Manning, G.; Whyte, D. B.; Martinez, R.; Hunter, T.; Sudarsanam, S. The Protein Kinase Complement of the Human Genome. *Science* **2002**, *298*, 1912–1934.
- (2) Blume-Jensen, P.; Hunter, T. Oncogenic Kinase Signalling. *Nature* **2001**, *411*, 355–365.
- (3) Holmgren, L.; O'Reilly, M. S.; Folkman, J. Dormancy of micrometastases: Balanced proliferation and apoptosis in the presence of angiogenesis suppression. *Nat. Med.* **1995**, *1*, 149–153.
- (4) Fukumura, D.; Xu, L.; Chen, Y.; Gohongi, T.; Seed, B.; Jain, R. K. Hypoxia and Acidosis Independently Up-Regulate Vascular Endothelial Growth Factor Transcription in Brain Tumors in Vivo. *Cancer Res.* **2001**, *61*, 6020–6024.
- (5) Dvorak, H. F. Vascular Permeability Factor/Vascular Endothelial Growth Factor: A Critical Cytokine in Tumor Angiogenesis and a Potential Target for Diagnosis and Therapy. *J. Clin. Oncol.* **2002**, *20*, 4368–4380.
- (6) Carmeliet, P. VEGF as a Key Mediator of Angiogenesis in Cancer. *Oncology* **2005**, *69* (Suppl. 3), 4–10.
- (7) Beck, L.; D'Amore, P. A. Vascular development: cellular and molecular regulation. *FASEB J.* **1997**, *11*, 365–373.
- (8) Reynolds, L. P.; Killilea, S. D.; Redmer, D. A. Angiogenesis in the female reproductive system. *FASEB J.* **1992**, *6*, 886–892.
- (9) Augustin, H. G. Antiangiogenic tumor therapy: will it work? *Trends Pharmacol. Sci.* **1998**, *19*, 216–222.
- (10) Ferrara, N.; Hillan, K. J.; Gerber, H.-P.; Novotny, W. Discovery and Development of Bevacizumab, an Anti-VEGF Antibody for Treating Cancer. *Nat. Rev. Drug Discovery* **2004**, *3*, 391–400.
- (11) Gschwind, A.; Fischer, O. M.; Ullrich, A. The Discovery of Receptor Tyrosine Kinases: Targets for Cancer Therapy. *Nat. Rev. Cancer* **2004**, *4*, 361–370.
- (12) Board, R.; Jayson, G. C. Platelet-Derived Growth Factor Receptor (PDGFR): A Target for Anticancer Therapeutics. *Drug Resist. Updates* **2005**, *8*, 75–83.
- (13) Sun, L.; Tran, N.; Tang, F.; App, H.; Hirth, P.; McMahon, G.; Tang, C. Synthesis and Biological Evaluations of 3-Substituted Indolin-2-ones: A Novel Class of Tyrosine Kinase Inhibitors That Exhibit Selectivity toward Particular Receptor Tyrosine Kinases. *J. Med. Chem.* **1998**, *41*, 2588–2603.
- (14) Laird, A. D.; Vajkoczy, P.; Shawver, L. K.; Thurnher, A.; Liang, C.; Mohammadi, M.; Schlessinger, J.; Ullrich, A.; Hubbard, S. R.; Blake, R. A.; Fong, T. A. T.; Strawn, L. M.; Sun, L.; Tang, C.; Hawtin, R.; Tang, F.; Shenoy, N.; Hirth, K. P.; McMahon, G.; Cherrington, J. M. SU6668 Is a Potent Antiangiogenic and Antitumor Agent That Induces Regression of Established Tumors. *Cancer Res.* **2000**, *60*, 4152–4160.
- (15) Fong, T. A. T.; Shawver, L. K.; Sun, L.; Tang, C.; App, H.; Powell, T. J.; Kim, Y. H.; Schreck, R.; Wang, X.; Risau, W.; Ullrich, A.; Hirth, K. P.; McMahon, G. SU5416 Is a Potent and Selective Inhibitor of the Vascular Endothelial Growth Factor Receptor (Flk-1/KDR) That Inhibits Tyrosine Kinase Catalysis, Tumor Vascularization, and Growth of Multiple Tumor Types. *Cancer Res.* **1999**, *59*, 99–106.
- (16) Sun, L.; Tran, N.; Liang, C.; Hubbard, S.; Tang, F.; Lipson, K.; Schreck, R.; Zhou, Y.; McMahon, G.; Tang, C. Identification of Substituted 3-[(4,5,6,7-Tetrahydro-1H-indol-2-yl)methylene]-1,3-dihydroindol-2-ones as Growth Factor Receptor Inhibitors for VEGF-R2 (Flk-1/KDR), FGF-R1, and PDGF-R $\beta$  Tyrosine Kinases. *J. Med. Chem.* **2000**, *43*, 2655–2663.
- (17) Klebl, B. M.; Müller, G. Second-generation kinase inhibitors. *Expert Opin. Ther. Targets* **2005**, *9*, 975–993.
- (18) Hicklin, D. J.; Ellis, L. M. Role of the Vascular Endothelial Growth Factor Pathway in Tumor Growth and Angiogenesis. *J. Clin. Oncol.* **2005**, *23*, 1011–1027.
- (19) Casanovas, O.; Hicklin, D. J.; Bergers, G.; Hanahan, D. Drug Resistance by Evasion of Antiangiogenic Targeting of VEGF Signaling in Late-Stage Pancreatic Islet Tumors. *Cancer Cell* **2005**, *8*, 299–309.
- (20) Sun, L.; Liang, C.; Shirazian, S.; Zhou, Y.; Miller, T.; Cui, J.; Fukuda, J. Y.; Chu, J.-Y.; Nematalla, A.; Wang, X.; Chen, H.; Sista, A.; Luu, T. C.; Tang, F.; Wei, J.; Tang, C. Discovery of 5-[5-Fluoro-2-oxo-

- 1,2-dihydroindol-(3Z)-ylidenemethyl]-2,4-dimethyl-1H-pyrrole-3-carboxylic Acid (2-Dimethylaminoethyl)amide, a Novel Tyrosine Kinase Inhibitor Targeting Vascular Endothelial and Platelet-Derived Growth Factor Receptor Tyrosine Kinase. *J. Med. Chem.* **2003**, *46*, 1116–1119.
- (21) Wilhelm, S. M.; Carter, C.; Tang, L.; Wilkie, D.; McNabola, A.; Rong, H.; Chen, C.; Zhang, X.; Vincent, P.; McHugh, M.; Cao, Y.; Shujath, J.; Gawlak, S.; Eveleigh, D.; Rowley, B.; Liu, L.; Adnane, L.; Lynch, M.; Auclair, D.; Taylor, I.; Gedrich, R.; Voznesensky, A.; Riedl, B.; Post, L. E.; Bollag, G.; Trail, P. A. BAY 43-9006 Exhibits Broad Spectrum Oral Antitumor Activity and Targets the RAF/MEK/ERK Pathway and Receptor Tyrosine Kinases Involved in Tumor Progression and Angiogenesis. *Cancer Res.* **2004**, *64*, 7099–7109.
- (22) Dai, Y.; Guo, Y.; Frey, R. R.; Ji, Z.; Curtin, M. L.; Ahmed, A. A.; Albert, D. H.; Arnold, L.; Arries, S. S.; Barlozzari, T.; Bauch, J. L.; Bouska, J. J.; Bousquet, P. F.; Cunha, G. A.; Glaser, K. B.; Guo, J.; Li, J.; Marcotte, P. A.; Marsh, K. C.; Moskey, M. D.; Pease, L. J.; Stewart, K. D.; Stoll, V. S.; Tapang, P.; Wishart, N.; Davidsen, S. K.; Michaelides, M. R. Thienopyrimidine Ureas as Novel and Potent Multitargeted Receptor Tyrosine Kinase Inhibitors. *J. Med. Chem.* **2005**, *48*, 6066–6083.
- (23) Curtin, M. L.; Frey, R. R.; Heyman, H. R.; Sarris, K. A.; Steinman, D. H.; Holms, J. H.; Bousquet, P. F.; Cunha, G. A.; Moskey, M. D.; Ahmed, A. A.; Pease, L. J.; Glaser, K. B.; Stewart, K. D.; Davidsen, S. K.; Michaelides, M. R. Isoindolinone Ureas: A Novel Class of KDR Kinase Inhibitors. *Bioorg. Med. Chem. Lett.* **2004**, *14*, 4505–4509.
- (24) (a) Albert, D. H.; Tapang, P.; Magoc, T. J.; Pease, L. J.; Reuter, D. R.; Wei, R.-Q.; Li, J.; Guo, J.; Bousquet, P. F.; Ghoreishi-Haack, N. S.; Wang, B.; Bukofzer, G. T.; Wang, Y.-C.; Stavropoulos, J. A.; Hartandi, K.; Niquette, A. L.; Soni, N.; Johnson, E. F.; McCall, J. O.; Bouska, J. J.; Luo, Y.; Donawho, C. K.; Dai, Y.; Marcotte, P. A.; Glaser, K. B.; Michaelides, M. R.; Davidsen, S. K. Preclinical activity of ABT-869, a multitargeted receptor tyrosine kinase inhibitor. *Mol. Cancer Ther.* **2006**, *5*, 995–1006. (b) Dai, Y.; Hartandi, K.; Ji, Z.; Ahmed, A. A.; Albert, D. H.; Bauch, J. L.; Bouska, J. J.; Bousquet, P. F.; Cunha, G. A.; Glaser, K. B.; Harris, C. M.; Hickman, D.; Guo, J.; Li, J.; Marcotte, P. A.; Marsh, K. C.; Moskey, M. D.; Martin, R. L.; Olson, A. M.; Osterling, D. J.; Pease, L. J.; Soni, N. B.; Stewart, K. D.; Stoll, V. S.; Tapang, P.; Reuter, D. R.; Davidsen, S. K.; Michaelides, M. R. Discovery of *N*-(4-(3-Amino-1*H*-indazol-4-yl)phenyl)-*N'*-(2-fluoro-5-methylphenyl)urea (ABT-869), a 3-Aminoindazole-Based Orally Active Multitargeted Receptor Tyrosine Kinase Inhibitor. *J. Med. Chem.* **2007**, *50*, 1584–1597.
- (25) The development of RTK inhibitors in the clinic has been extensively reviewed. For recent reviews, see the following: (a) Arora, A.; Scholar, E. M. Role of Tyrosine Kinase Inhibitors in Cancer Therapy. *J. Pharmacol. Exp. Ther.* **2005**, *315*, 971–979. (b) Laird, A. D.; Cherrington, J. M. Small Molecule Tyrosine Kinase Inhibitors: Clinical Development of Anticancer Agents. *Expert Opin. Invest. Drugs* **2003**, *12*, 51–64. (c) Manley, P. W.; Bold, G.; Brügger, J.; Fendrich, G.; Furet, P.; Mestan, J.; Schnell, C.; Stolz, B.; Meyer, T.; Meyhack, B.; Stark, W.; Strauss, A.; Wood, J. Advances in the Structural Biology, Design and Clinical Development of VEGF-R Kinase Inhibitors for the Treatment of Angiogenesis. *Biochim. Biophys. Acta* **2004**, *1697*, 17–27.
- (26) Traxler, P.; Furet, P. Strategies toward the Design of Novel and Selective Protein Tyrosine Kinase Inhibitors. *Pharmacol. Ther.* **1999**, *82*, 195–206.
- (27) Bold, G.; Florsheimer, A.; Furet, P.; Imbach, P.; Masuya, K.; Schoepfer, R. Scientists at Novartis have independently discovered 7-amino-pyrazolo[1,5-*a*]pyrimidine ureas as kinase inhibitors: Organic compounds, US2005/0222171 A1, 2005.
- (28) Alcade, E.; deMendoza, J.; Garcia-Marquina, J. M.; Almera, C.; Elguero, J. Etude de la Réaction du  $\beta$ -Aminocrotonitrile et du  $\alpha$ -Formyl Phénylacétonitrile avec l'Hydrazine: Synthèse d'Amino-7-pyrazolo[1,5-*a*]pyrimidines. *J. Heterocycl. Chem.* **1974**, *11*, 423–429.
- (29) Miyaura, N.; Suzuki, A. Palladium-Catalyzed Cross-Coupling Reactions of Organoboron Compounds. *Chem. Rev.* **1995**, *95*, 2457–2483.
- (30) Fraley, M. E.; Hoffman, W. F.; Rubino, R. S.; Hungate, R. W.; Tebben, A. J.; Rutledge, R. Z.; McFall, R. C.; Huckle, W. R.; Kendall, R. L.; Coll, K. E.; Thomas, K. A. Synthesis and Initial SAR Studies of 3,6-Disubstituted Pyrazolo[1,5-*a*]pyrimidines: A New Class of KDR Kinase Inhibitors. *Bioorg. Med. Chem. Lett.* **2002**, *12*, 2767–2770.
- (31) Nam, N. L.; Grandberg, I. I.; Sorokin, V. I. Pyrazolopyrimidines Based on 5-Aminopyrazoles Unsubstituted at the Position 1. *Chem. Heterocycl. Compd.* **2002**, *38*, 1371–1374.
- (32) Gribble, F. M.; Loussouarn, G.; Tucker, S. J.; Zhao, C.; Nichols, C. G.; Ashcroft, F. M. A Novel Method for Measurement of Submembrane ATP Concentration. *J. Biol. Chem.* **2000**, *275*, 30046–30049.
- (33) Miyazaki, Y.; Matsunaga, S.; Tang, J.; Maeda, Y.; Nakano, M.; Philippe, R. J.; Shibahara, M.; Liu, W.; Sato, H.; Wang, L.; Nolte, R. T. Novel 4-Amino-furo[2,3-*d*]pyrimidines as Tie-2 and VEGFR2 Dual Inhibitors. *Bioorg. Med. Chem. Lett.* **2005**, *15*, 2203–2207.
- (34) Fraley, M. E.; Rubino, R. S.; Hoffman, W. F.; Hambaugh, S. R.; Arrington, K. L.; Hungate, R. W.; Bilodeau, M. T.; Tebben, A. J.; Rutledge, R. Z.; Kendall, R. L.; McFall, R. C.; Huckle, W. R.; Coll, K. E.; Thomas, K. A. Optimization of a Pyrazolo[1,5-*a*]pyrimidine Class of KDR Kinase Inhibitors: Improvements in Physical Properties Enhance Cellular Activity and Pharmacokinetics. *Bioorg. Med. Chem. Lett.* **2002**, *12*, 3537–3541.
- (35) Aronov, A. M.; Baker, C.; Bemis, G. W.; Cao, J.; Chen, G.; Ford, P. J.; Germann, U. A.; Green, J.; Hale, M. R.; Jacobs, M.; Janetka, J. W.; Maltais, F.; Martinez-Botella, G.; Namchuk, M. N.; Straub, J.; Tang, Q.; Xie, X. Flipped Out: Structure-Guided Design of Selective Pyrazolylpyrrole ERK Inhibitors. *J. Med. Chem.* **2007**, *50*, 1280–1287.
- (36) Ma, W.; Tan, J.; Matsumoto, H.; Robert, B.; Abrahamson, D. R.; Das, S. K.; Dey, S. K. Adult Tissue Angiogenesis: Evidence for Negative Regulation by Estrogen in the Uterus. *Mol. Endocrinol.* **2001**, *15*, 1983–1992.
- (37) Inhibition values exceeding 30% were significantly different ( $p < 0.05$ ) from vehicle-treated controls.
- (38) Compound **34a** was screened against a wider panel of 150 kinases. At 1 mM ATP concentration, IC<sub>50</sub> values of <1000 nM were noted for TrkA (99 nM) and TrkB (52 nM). Kinases showing IC<sub>50</sub> < 1000 nM at lower ATP concentration included Src, Lck, JAK2, Abl, and Fyn. Without inhibition data at 1 mM ATP, however, it is not possible to make a direct comparison of these screening data with the data reported in Table 7.
- (39) Kolb, A. J.; Kaplita, P. V.; Hayes, D. J.; Park, Y.-W.; Pernel, C.; Major, J. S.; Mathis, G. Tyrosine Kinase Assays Adapted to Homogeneous Time-Resolved Fluorescence. *Drug Discovery Today* **1998**, *3*, 333–342.